

# The Parkes Half-Jansky Flat-Spectrum Sample

M. J. Drinkwater<sup>1</sup>, R. L. Webster<sup>2</sup>, P. J. Francis<sup>2</sup>, J. J. Condon<sup>3</sup>, S. L. Ellison<sup>4,1</sup>,  
D. L. Jauncey<sup>5</sup>, J. Lovell<sup>6</sup>, B. A. Peterson<sup>7</sup>, A. Savage<sup>1\*</sup>

<sup>1</sup>Anglo-Australian Observatory, Coonabarabran, New South Wales 2357, Australia

<sup>2</sup>School of Physics, University of Melbourne, Parkville, Victoria 3052, Australia

<sup>3</sup>National Radio Astronomy Observatory<sup>†</sup>, 520 Edgemont Road, Charlottesville, VA 22903, USA

<sup>4</sup>Physics Department, University of Kent at Canterbury, Canterbury, Kent CT2 7NP, England

<sup>5</sup>Australia Telescope National Facility, P.O. Box 76, Epping, New South Wales 2121, Australia

<sup>6</sup>Physics Department, University of Tasmania, GPO Box 252C, Hobart, Tasmania 7001, Australia

<sup>7</sup>Mt. Stromlo & Siding Spring Observatories, Australian National University, Private Bag, Weston Creek, A.C.T. 2611, Australia

This is a preprint of a paper accepted for publication in MNRAS.

## ABSTRACT

We present a new sample of Parkes half-Jansky flat-spectrum radio sources having made a particular effort to find any previously unidentified sources. The sample contains 323 sources selected according to a flux limit of 0.5 Jy at 2.7 GHz, a spectral index measured between 2.7 and 5.0 GHz of  $\alpha_{2.7/5.0} > -0.5$ , where  $S(\nu) \propto \nu^\alpha$ , Galactic latitude  $|b| > 20^\circ$  and  $-45^\circ < \text{Declination (B1950)} < +10^\circ$ . The sample was selected from a region 3.90 steradians in area.

We have obtained accurate radio positions for all the unresolved sources in this sample and combined these with accurate optical positions from digitised photographic sky survey data to check all the optical identifications. We report new identifications based on *R*- and *K<sub>n</sub>*-band imaging and new spectroscopic measurements of many of the sources. We present a catalogue of the 323 sources of which 321 now have identified optical counterparts and 277 have measured spectral redshifts.

**Key words:** catalogues — radio continuum: galaxies — BL Lac objects: general — galaxies: general — quasars: general

## 1 INTRODUCTION

The Southern sky was surveyed at 2.7 GHz by the Parkes radio telescope between 1968 and 1979 (see Bolton, Savage & Wright 1979, and references therein), resulting in a catalogue of more than 10,000 radio sources. Over this period, an extensive programme of optical identifications was undertaken. In its early stages, this programme was frustrated by lack of a Southern radio calibrator grid, poor radio positions (the original Parkes positions were only accurate to 10–15 arcsec) and a lack of optical sky survey plates. Modern methods, using accurate (better than 1 arcsec) radio positions and complete catalogues of digitised optical sky survey data, with the radio and optical reference frames tied to an accuracy of better than 100 milliarcsec (Johnston et

al. 1995) now allow unambiguous optical identification of most of the radio sources, supplemented by CCD imaging for the remainder. In this paper we present new identifications of a sample of Parkes flat-spectrum radio sources using these techniques. The Parkes Catalogue contains both steep- and flat-spectrum sources. Radio samples are biased towards core-dominated quasars if the flat-spectrum sources are selected and towards lobe-dominated quasars and galaxies for steep-spectrum sources. Since the scientific questions of primary interest to us are related to core-dominated quasars, we concentrate on flat-spectrum sources in this study.

Other workers have compiled a number of complete samples of radio sources. Each has been selected on different criteria, leading to the inclusion of different objects. Low frequency samples contain more radio galaxies than quasars, high frequency (i.e. flat-spectrum) samples reverse that bias, and lower flux limits increase the mean redshift of the objects in the sample. Four notable samples are the 3CR Sample (Spinrad et al. 1985, Laing, Riley & Longair 1983), the 2 Jansky Sample (Wall & Peacock 1985), the 1 Jansky Sample

\* Present address: “Holly Farm”, Binnaway Road, Coonabarabran, New South Wales 2357, Australia.

<sup>†</sup> The National Radio Astronomy Observatory is operated by Associated Universities, Inc., under cooperative agreement with the National Science Foundation.

(Kühr et al. 1981; Stickel, Meisenheimer & Kühr 1994), and the Parkes Selected Regions (Dunlop et al. 1989).

The 3CR sample comprises 173 sources selected with  $S_{178\text{ MHz}} > 10\text{ Jy}$  over an area of 4.23 Sr. The high flux limit biases this sample towards lower redshift objects (18% have  $z > 1$ ), and the use of a low frequency biases the sample towards steep-spectrum radio galaxies. The 2 Jansky sample, which was selected at 2.7 GHz over an area of 9.81 Sr, contains 233 objects which are mainly steep-spectrum, again biasing the sample towards low-redshift radio galaxies. The 1 Jansky sample was selected at 5 GHz, also over 9.81 Sr of sky and comprises 518 sources. 55% are flat-spectrum sources, and of those  $\sim 90\%$  are quasars or BL Lacs; many are Parkes sources. Finally, the Parkes Selected Regions (a total of 0.075 Sr) contain 178 sources with  $S_{2.7\text{ GHz}} > 0.1\text{ Jy}$ , most of which are steep-spectrum extended sources identified as galaxies. Only 23% are flat-spectrum sources, but these objects have a distribution of properties similar to our sample.

Our primary interest in this paper is the compilation of a large unbiased sample of radio-selected quasars. Note that we use the standard definitions of “quasar” for radio-loud sources and quasi-stellar-object (QSO) for optically-selected sources. There were several motivations for defining the sample. First, we were interested in using quasars for gravitational lensing studies. A proper determination of lensing statistics requires the identification of complete quasar samples, as well as an understanding of any selection effects which might bias selection of gravitationally lensed quasars. Secondly, the recent completion of the Large Bright QSO Survey (LBQS; Hewett, Foltz & Chaffee 1995) has meant that there is a well-defined sample of optically-selected QSOs, allowing the determination of global spectroscopic properties. The completion of a comparable sample of radio-selected quasars will allow a detailed phenomenological comparison of the optical spectra of these two classes of object, perhaps allowing the determination of differences in underlying physical conditions. Finally, quasars are one of the most effective probes of the universe to high redshift, providing a measure of evolution as well as the formation of large-scale structure. Of course the complete identification of a sample of radio sources can also provide some surprises, if unexpected objects, such as very high redshift quasars, are found.

The Parkes Half-Jansky Flat-spectrum Sample we define here contains 323 sources selected in an area of 3.90 Sr and is similar to the earlier compilation by Savage et al. (1990). We have made significant progress in the optical identification of the sources which were previously termed “Empty Fields”, particularly by using near infrared  $K_n$  band (2.0–2.3 microns) imaging to detect the optically faint sources. The extremely red optical to near infrared colours of these sources imply that most are heavily reddened, viewed through dust either in the line-of-sight to the quasar or within the immediate quasar environment (see Webster et al. 1995). In this paper we present optical identifications for 321 sources (99% of the sample), and redshifts for 277 sources (86%).

The outline of the paper is as follows. The selection criteria for the radio sources are described in Section 2. In Section 3 we explain how the accurate radio positions were obtained, and present radio images of the resolved sources in

the sample. Section 4 describes the mapping of the accurate radio positions onto the optical catalogues. We present a full discussion of the accuracy of this procedure, locate the likely optical counterparts, classify these images as either stellar or non-stellar and provide the optical magnitudes. Where there is no optical survey image at the location of the radio source, we use R-band CCD frames and  $K_n$  near infrared images to determine the source identification and morphology. In Section 5 we present spectroscopic classifications and redshifts of these sources; for those sources which do not have a published spectrum, we also include the spectra. All these results are summarised in a master catalogue of the sample in Section 6. Finally, Section 7 presents a summary of the most important features of our sample. An electronic version of our catalogue is available from the Centre de Données astronomiques de Strasbourg in Section VIII (“Radio Data”) of the catalogue archive.

## 2 SELECTION OF THE SAMPLE

### 2.1 Radio Surveys

Our basic selection criteria are very similar to those used by Savage et al. (1990). We started with the machine-readable version of the Parkes catalogue (PKSCAT90, Wright & Otrupcek 1990) and applied the following criteria:

- (i) 2.7 GHz ( $S_{2.7}$ ) and 5.0 GHz ( $S_{5.0}$ ) fluxes defined
- (ii)  $S_{2.7} > 0.5\text{ Jy}$
- (iii) spectral index  $\alpha_{2.7/5.0} > -0.5$ , where  $S(\nu) \propto \nu^\alpha$
- (iv) Galactic latitude  $|b| > 20^\circ$
- (v)  $-45^\circ < \text{Declination (B1950)} < +10^\circ$

In our search of PKSCAT90, three objects did not have a 5.0 GHz flux defined but satisfied all the other criteria. One of these was later included from our search of the discovery papers, but the other objects were not measured at 5.0 GHz in the discovery papers, presumably because they are very bright radio sources associated with bright optical galaxies: PKS 0131–367 (5.6 Jy, 15mag) and PKS 0320–374 (98 Jy, 10mag) and were too extended to measure properly. This search resulted in an initial sample of 325 objects.

We then carefully checked all the radio fluxes in the original discovery papers of the radio survey, as listed in Table 1. Many objects have more recent (but unreferenced) flux measurements listed in PKSCAT90, but we replaced these with the original fluxes in order to quantify the time difference between the 2.7 and 5.0 GHz measurements and thus estimate the effects of variability. After the original fluxes were adopted, 15 sources no longer satisfied the flux and spectral criteria and so were excluded. We also found 17 sources whose original fluxes in the discovery papers satisfied the selection criteria so these were added to the sample.

In two regions (samples A and F; see Table 1) our search of PKSCAT90 produced several sources not listed in the original papers. These two regions of the original survey were not complete because the flux limit was not well-defined; subsequent unpublished observations detected additional sources satisfying our selection criteria that were included in PKSCAT90. We retained these additional objects (12 in each region), but flagged them with a minus sign in front of the reference code (Rf) in the final catalogue (Table 5).

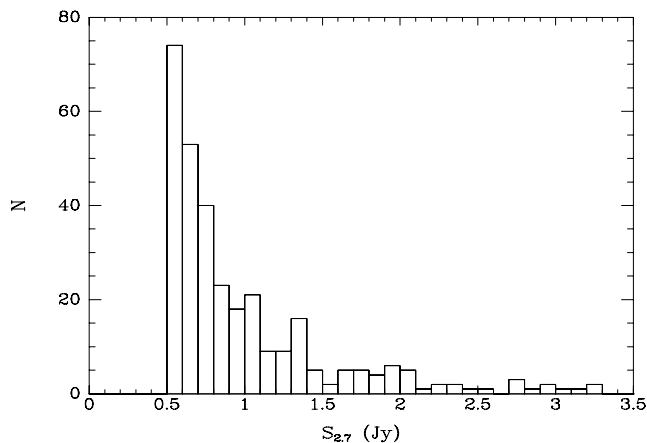


**Figure 1.** Histogram of the 2.7 GHz fluxes of the sources in the sample.

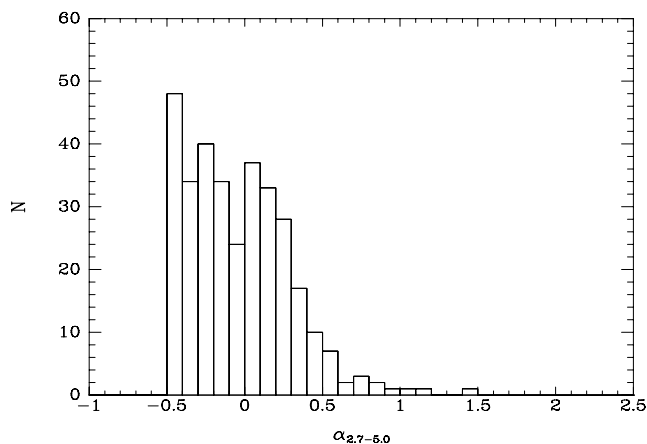


**Figure 2.** Histogram of the (2.7 to 5.0 GHz) radio spectral indices of the sample sources ( $S(\nu) \propto \nu^\alpha$ ).

Finally we removed four planetary nebulae from the sample on the basis that we are interested in extragalactic sources. This gave a final sample of 323 sources which are listed in Table 5 in Section 6. Our new sample is complete in 6 of the 8 sub-regions listed in Table 1 but in two of the regions (A and F) the original surveys are incomplete and we have added additional sources from PKSCAT90. The distributions of the fluxes and spectral indices are given in Figs. 1 and 2 respectively and a diagram showing the regions surveyed and the distribution of our sample across the sky is shown in Fig. 3.

## 2.2 Variability

Flat-spectrum radio sources are well-known to be variable, which introduces two biases in our sample. First, our sample was selected to have a 2.7 GHz flux above 0.5 Jy *at the observation epoch*. Some of the sample may have been in a particularly bright state; their average fluxes may be below our limit. Likewise some flat-spectrum sources with average fluxes above 0.5 Jy may have been excluded from the sample because they were in a particularly faint state when the

sample was defined. Secondly, the 5 GHz observations of the sample sources were not obtained simultaneously with the 2.7 GHz observations (see Table 1). The 5 GHz observations were usually taken after the 2.7 GHz observations; the time interval being more than 6 months in  $\sim 40\%$  of cases; six months is a typical variability timescale for compact radio sources (Fiedler et al. 1987). If a source varied between the two observations, its spectral index could be in error, and the object might be wrongly included in, or excluded from, the flat-spectrum sample.

Stannard & Bentley (1977) investigated the variability of 50 Parkes flat-spectrum radio sources, substantially overlapping our sample. They compared 2.7 GHz fluxes taken two years apart, and found that  $\sim 50\%$  of sources had varied by 15% or more. The number of sources included in the flux limited sample because they were brighter than average at the time of observation will exceed the number of sources missed because they were fainter than average. This is because there are more sources with mean fluxes just below 0.5 Jy than there are with fluxes just above 0.5 Jy, due to the steepness of the number/flux relation. Using Stannard & Bentley’s numbers, we estimate that  $\sim 30$ – $40$  of our sources have mean fluxes below 0.5 Jy, and that we missed  $\sim 20$ – $30$  sources with mean fluxes above 0.5 Jy.

Allowing for the time delay between the 2.7 GHz and 5 GHz measurements, we can also estimate that  $\sim 10$  flat-spectrum sources with  $-0.5 < \alpha < -0.3$  will have been mistakenly classified as steep-spectrum and excluded from our sample, while another  $\sim 10$  with  $-0.7 < \alpha < -0.5$  will have been wrongly included. This calculation ignores the dependence of variability on spectral index. Fiedler et al. (1987) showed that most bright compact radio sources with relatively steep-spectra ( $\alpha < -0.2$ ) vary by only  $\sim 5\%$  on timescales of two years. This implies that we will only misclassify  $\sim 5$  objects with  $-0.5 < \alpha < -0.3$  as being steep-spectrum. However, they also find that a small fraction of very flat-spectrum sources ( $\alpha > -0.2$ ) can vary by 50% or more on timescales of two years. Applying their numbers to our sample, we estimate that  $\sim 2$  sources with  $\alpha > -0.2$  may have varied by enough to have been misclassified as steep-spectrum. These numbers may be an overestimate; Fiedler et al. only considered compact sources, whereas several of our objects, particularly those with steeper spectra, are extended and may be less variable. We plan to address this uncertainty by remeasuring the sample making simultaneous flux measurements at both frequencies.

In summary, variability imposes an uncertainty on our 0.5 Jy completeness limit at 2.7 GHz: some 30–40 ( $\sim 11\%$ ) sources in our sample have mean fluxes below the limit, and we missed some 20–30 ( $\sim 8\%$ ) sources with mean fluxes above the limit. This bias is inherent to any single-epoch flux-limited sample.

On the other hand we find that  $\sim 5$ – $10$  objects in our sample actually have  $\alpha < -0.5$  (steep-spectrum) and have been wrongly included because they varied between the epochs of the 2.7 GHz and 5.0 GHz measurements, but that another  $\sim 5$ – $10$  flat-spectrum objects were missed for the same reason.

**Table 1.** The Parkes Survey Regions

Region	Dec range	RA range	$\Delta T^1$ month	Flux Limit $S_{2.7}(\text{Jy})$	Reference (code)	$N^2$
A	+10°, +04°	7 <sup>h</sup> -18 <sup>h</sup> , 20 <sup>h</sup> 30-5 <sup>h</sup> 30	2,9	$\approx 0.5^3$	Shimmins, Bolton & Wall (1975) (79)	46
B	+04°, -04°	7 <sup>h</sup> 20-17 <sup>h</sup> 50, 19 <sup>h</sup> 40-6 <sup>h</sup>	2-9	0.35	Wall, Shimmins & Merkelijn (1971) <sup>4</sup> (102)	63
C	-04°, -15°	10 <sup>h</sup> -15 <sup>h</sup>	2-14	0.25	Bolton, Savage & Wright (1979) (8)	21
D	-15°, -30°	10 <sup>h</sup> -15 <sup>h</sup>	3	0.25	Savage, Wright & Bolton (1977) (70)	34
E	-04°, -30°	22 <sup>h</sup> -5 <sup>h</sup>	1-12	0.22	Wall, Wright & Bolton (1976) (103)	65
F	-04°, -30°	5 <sup>h</sup> -6 <sup>h</sup> 30, 8 <sup>h</sup> -10 <sup>h</sup> , 15 <sup>h</sup> -17 <sup>h</sup> , 19 <sup>h</sup> -22 <sup>h</sup>	2-9	$\approx 0.6^3$	Bolton, Shimmins & Wall (1975) (7)	39
G	-30°, -35°	9 <sup>h</sup> -16 <sup>h</sup> 30, 18 <sup>h</sup> 30-7 <sup>h</sup> 15	1-10	0.18	Shimmins & Bolton (1974) (78)	25
H	-35°, -45°	10 <sup>h</sup> -15 <sup>h</sup> , 19 <sup>h</sup> -7 <sup>h</sup>	9	0.22	Bolton & Shimmins (1973) (6)	30
					total	323

Notes: 1.  $\Delta T$  is the time delay between the 2.7 and 5.0 GHz measurements. 2.  $N$  is the number of sources each region contributes to our sample. 3. No completeness analysis was made for regions A and F so extra objects from PKSCAT90 not in the original papers were included (12 in each case) and the flux limits are only indicative. 4. The 5 GHz fluxes for region B were published separately by Wall (1972).

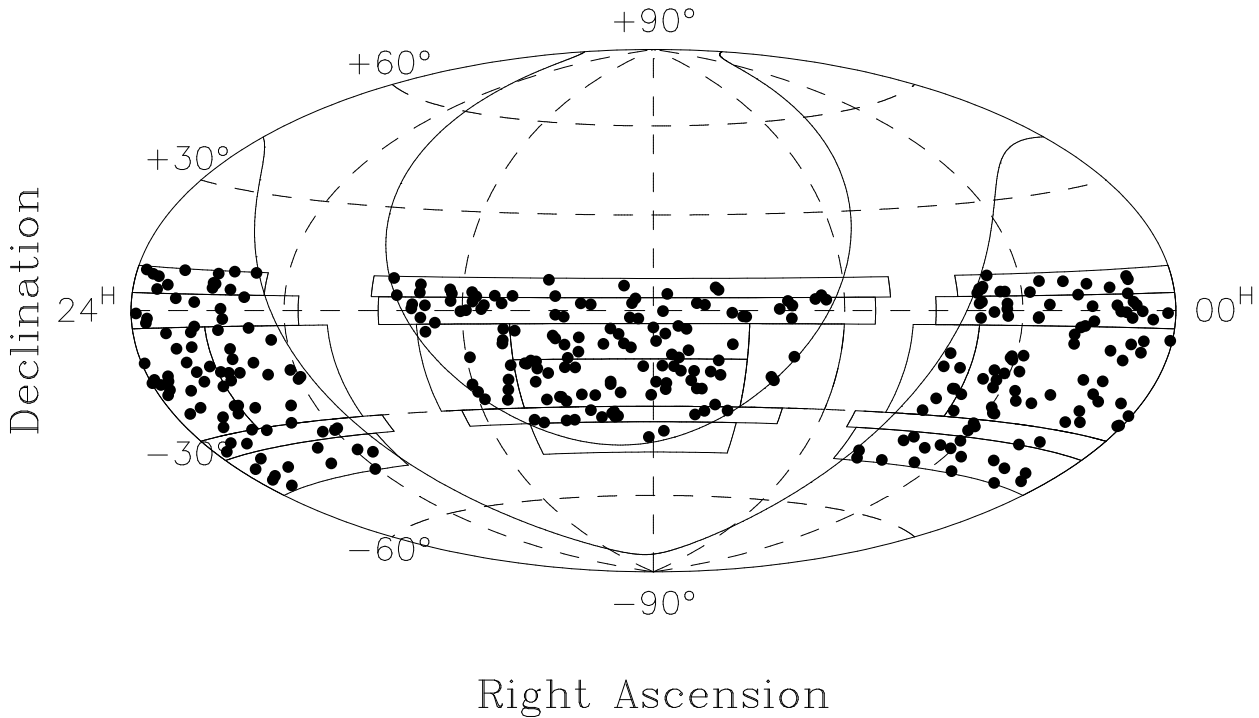


**Figure 3.** Distribution on the sky of The Parkes Half-Jansky Flat-Spectrum Sample (equal-area projection). The solid lines indicate the the survey regions and the limits of Galactic latitude ( $|b| > 20^\circ$ ).

### 3 RADIO POSITIONS

We had to improve on the poor (10–20 arcsec) accuracy of the original Parkes radio positions before being able to make optical identifications of the radio sources by positional coincidence. To this end we have obtained more accurate radio positions for all sources in the sample using published data, The VLA Calibrator Manual (as compiled by Perley & Taylor, 1996) and our own Very Large Array (VLA) and Australia Telescope Compact Array (ATCA) observations. The sources of these positions and the associated errors are listed in Table 2. The source positions are listed in Table 5; note that we use the original naming scheme for the sources based on B1950 coordinates but we include the J2000 coordinates for all the sources in Table 5 for reference.

#### 3.1 VLA Observations and Data Reduction

On 1986 October 1 and 4 we observed the majority of the sources that lacked accurate published positions with the VLA. The observations were made at 4.86 GHz with the VLA in its “CnB” configuration to yield nearly circular synthesised beams with approximately 6 arcsec FWHM resolution. Each programme source was covered with a single “snapshot” scan of about 3 minutes duration, and each group of snapshots was preceded and followed by scans on a phase calibrator whose rms absolute position uncertainty is not more than 0.1 arcsec in each coordinate. The phase calibrator flux densities were bootstrapped to the Baars et al. (1977) scale via observations of 3C 48 and 3C 286.

The (u,v) data recorded from both circular polariza-

**Table 2.** Sources of accurate radio positions

Reference (code)	uncertainty (arcsec)
Jauncey et al. (1989) (39)	0.15
Johnston et al. (1995) (40)	0.01
Lister et al. (1994) (43)	$\approx 0.3$
Ma et al. (1990) (45)	0.01
Morabito et al. (1982) (50)	0.6
Patnaik (1996) (55)	$\approx 0.02$
Perley (1982) (56)	0.15
Perley & Taylor (1996) (57)	$\approx 0.15$
Preston et al. (1985) (60)	0.6
Ulvestad et al. (1981) (97)	0.40
This paper: ATCA (120)	0.0-0.3
This paper: VLA (121)	0.2-0.5

tions in two 50 MHz bands centered on 4.835 and 4.885 GHz were edited, calibrated, and mapped with AIPS. The images were cleaned, and the clean components were used to self-calibrate the antenna phases, yielding images with dynamic ranges typically  $> 200 : 1$ . Nearly every programme source contains a dominant compact component that should coincide in position with any possible optical identification. The positions of these compact components were determined by Gaussian fitting on the images. The formal fitting residuals were  $< 0.1$  arcsec because the synthesised beam is small and the signal-to-noise ratios are high. Thus the radio position uncertainties are dominated by atmospheric phase drifts and gradients not removed by the calibration. They range from about 0.2 arcsec at Dec  $+10^\circ$  to about 0.5 arcsec at Dec  $-45^\circ$ .

### 3.2 ATCA Observations and Data Reduction

Several remaining sources in the sample were observed with the ATCA during 1993 March and November using all 6 antennas with a maximum baseline of 6 km. Observations were made at 4.80 and 8.64 GHz in “cuts” mode with orthogonal linear polarisations at a bandwidth of 128 MHz. The synthesised beam at 4.80 GHz has a constant East-West resolution of 2 arcsec FWHM and a North-South resolution varying from 3 arcsec (at Dec  $-45^\circ$ ) to 8 arcsec (Dec  $-21^\circ$ ). “Cuts” mode involves observing each object for a period of one minute on at least 6 occasions spread evenly over 12 hours. In this way, it is possible to obtain imaging data on approximately 40 sources within a 12 hour observation. Secondary calibrators with accurate, milliarcsec positions close to the programme sources were observed at least once every 2 hours. The flux density scale was determined from observations of the primary calibrator at the ATCA, PKS 1934–638.

The data were edited and calibrated within AIPS and images made using the Caltech Difmap software (Shepherd, Pearson & Taylor, 1995). The final self-calibrated images have typical dynamic ranges in excess of 400:1 for strong and relatively compact sources, decreasing to approximately 100:1 for objects with weak or extended emission. Source positions were calculated by fitting a Gaussian to the peak in the brightness distribution of a cleaned (but not self-calibrated) 8.64 GHz image. The uncertainty in source positions measured from these ATCA images comprises a com-

ponent due to thermal noise, which scales inversely with S/N ( $\sim \text{beamwidth}/(S/N)$ ) and a component due to systematic effects arising from the phase-referencing. The latter term dominates for strong sources and scales linearly with angular distance between the source and the phase-reference used to calibrate its position. The error is approximately 0.1 arcsec for an angular separation of  $5^\circ$  (Reynolds et al. 1995).

### 3.3 The Radio Positions and Morphology

The new radio positions are presented in Table 5. As shown in Table 2 these are all accurate to 0.6 arcsec or better for unresolved sources. Any radio sources we know to be resolved are noted in the comments column of Table 5 and we present radio images of these sources in Fig. A1. We indicate five different categories of resolved source in the Table using the terminology of Downes et al. (1986):

- (i) “P” signifies partially resolved sources: the position is well-defined by a peak.
- (ii) “Do” indicates double sources with no central component or dominant peak. There is no clear maximum, so the centroid of the image was used to define the position.
- (iii) “Do+CC” indicates a double-lobed source with a central component or peak that gives a well-defined position.
- (iv) “H” indicates a diffuse halo around a central source which gives a well-defined position.
- (v) “HT” indicates a complex head-tail structure with no well-defined position.

### 3.4 Notes on Individual Radio Positions

In this section we describe any sources with extended structure making the position difficult to define. We also note any sources for which our final accurate positions differ by more than 24 arcsec from the original Parkes catalogue positions.

(i) PKS 0114+074: there are 3 components to the VLA radio image in Fig. A1. We have adopted the centroid of the stronger double source to the South, although the Northern source also has an optical counterpart. The PKSCAT90 position corresponds to the Northern source; our position is therefore some 30 arcsec different. Our spectroscopic observations show that the Northern source (at 01:14:49.51 +07:26:30.0 B1950) is a broad-lined quasar at  $z = 0.858$  consistent with previous publications. The correct identification (at 01:14:50.48 +07:26:00.3 B1950) is a narrow-line galaxy at  $z = 0.342$ .

(ii) PKS 0130–447: this position is some 30 arcsec from the original value.

(iii) PKS 0349–278: the VLA image in Fig. A1 is confused with a compact source some 2.5 arcmin from the PKSCAT90 position and a marginal detection at the PKSCAT90 position. We made an independent check of the radio centroid position for this source by measuring it on the 4.85 GHz survey images made with the NRAO 140-foot telescope (Condon, Broderick & Seielstad, 1991). A Gaussian fit gave a position of 03:49:31.5 –27:53:41 (B1950), consistent with the original position (and coincident with an optical galaxy) but not with the stronger VLA source at 03:49:41.17 –27:52:07.0 (B1950). Furthermore, the fit is

clearly extended (source size 280 arcsec by 109 arcsec with position angle  $50^\circ$  after the beam has been deconvolved). The 4.85 GHz flux of PKS 0349–278 is just over 2 Jy, but the strong source in the VLA image is only 0.3 Jy. The VLA has resolved out most of the flux, leaving only two components plus some residuals visible in the contour plot. The strong VLA component is probably only a hotspot in the northeastern lobe of the radio source. We adopt the fainter VLA position (03:49:31.81 –27:53:31.5 B1950) which is consistent with the single-dish positions.

(iv) PKS 0406–311: the VLA image in Fig. A1 shows a complex head-tail source with no clear centre. The Northern limit of the source is close to a bright galaxy. We tentatively claim this as the identification, although the separation is 7.25 arcsec from the poorly defined “head” of the radio source and about 35 arcsec from the original position.

(v) PKS 0511–220: we find a very large difference between our position for this source (05:11:41.81 –22:02:41.2, B1950) and that quoted in Hewitt & Burbidge (1993) (05:11:49.94 –22:02:44.8). We attribute this difference to a typographical error made with respect to the position (05:11:41.94 –22:02:44.8) given by Condon, Hicks & Jauncey (1977). We are concerned that any published redshifts of this object may correspond to an object near the wrong position so we do not quote a redshift for this source pending our own observations.

(vi) PKS 1008–017: (see Fig. A1) our new position is about 40 arcsec from the original value.

(vii) PKS 1118–056: this is 60 arcsec away from the original survey position; we suspect a typographical error in the discovery paper (Bolton et al. 1979).

(viii) PKS 2335–181: in the case of this double source (see Fig. A1) with no central component the centroid of the image was not used to define the position; the North-East component was adopted instead. This was chosen because of the very good positional correspondence with a quasar at redshift  $z=1.45$  and also the fact that no optical counterpart for the South-West component was detected in the Hubble Space Telescope Snapshot Survey (Maoz et al. 1993).

## 4 OPTICAL IDENTIFICATIONS

### 4.1 Matching to Sky Survey Positions

A major advance that we present in this paper is the matching of our accurate radio source positions to the accurate optical data now available in large digitised sky catalogues based on the U.K. Schmidt Telescope (UKST) and Palomar sky surveys. A factor contributing to our successful identifications is the greatly improved agreement between the radio and optical reference frames in the South (e.g. Johnston et al. 1995).

Our major source of optical data is the COSMOS/UKST Southern Sky Catalogue. This lists image parameters derived from automated measurements of the ESO/SERC Southern Sky Survey plates, taken on IIIa-J emulsion with the GG395 filter to give the photographic blue passband  $B_J$  (3950–5400 Å). The catalogue is described further by Yentis et al. (1992). There are systematic errors in the astrometry of the COSMOS catalogue: we made a first-order correction as described by Drinkwater, Barnes &

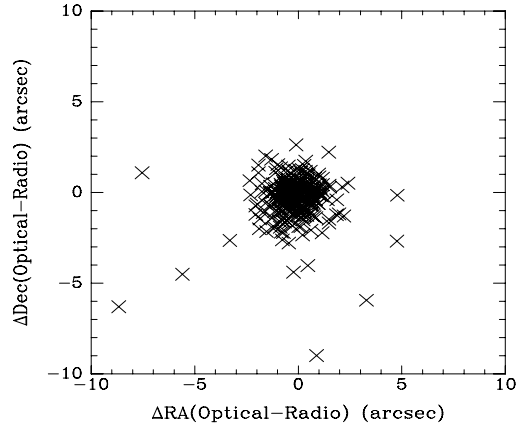


**Figure 4.** Distribution of the Position Offsets between each radio source position and the nearest detected image in the sky catalogues.

Ellison (1995) by using the PPM star catalogue (Röser, Bastian & Kuzmin 1994) to calculate a mean shift in the positions for each Schmidt field used.

For sources North of +3 degrees we used data from the Automated Plate Measuring facility (APM; see Irwin, Maddox & McMahon 1994) at Cambridge based on blue (unfiltered 103a-O emulsion; 3550–4650 Å) and red (red plexiglass 2444 filter plus 103a-E emulsion; 6250–6750 Å) plates from the first Palomar Observatory Sky Survey (POSS I).

The sky catalogues were used to generate finding charts for all the sources which we present in Appendix B. These charts are a good approximation to the photographic data, but we stress that there can be problems with image merging in crowded fields: close objects (e.g. two stars) can be misclassified as a “merged” object or galaxy. The “Field” code at the bottom of each chart indicates the UKST field number (or the plate number for POSS I) with a prefix describing the type of plate. The prefix “J” indicates UKST  $B_J$  plates measured by COSMOS. For APM data “j” indicates UKST  $B_J$  plates, “O” blue POSS I plates and “E” red POSS I plates.

The procedure to find the optical counterpart to each radio source started with the selection of the nearest optical image in the catalogues to each radio position. The relative positions of these nearest-neighbours are shown in Fig. 4. There is a clear concentration at small separations (less than 3 arcsec), but we note that in some cases the nearest-neighbours are at larger separations (greater than 5 arcsec). We made a preliminary estimate of the spread in the position offsets by fitting Gaussians to the distributions in RA and Dec; the rms scatter was found to be about 0.9 arcsec in each direction. A preliminary cutoff separation of 4 arcsec (about  $4\sigma$ ) was then imposed.

We removed the outliers more distant than 4 arcsec and then recalculated the distributions of position offsets: these are shown plotted in Fig. 5 as histograms of the offsets between the two positions in RA and Dec. We estimated the statistical range of this distribution by measuring the Gaussian dispersions in RA and Dec. These results are given in Table 3. This shows that the core of the distribution has dispersions of only about 0.8 arcsec in each direction. (The

**Table 3.** Mean Optical–Radio Position Offsets

sample	N	$\overline{\Delta RA}$ arcsec	$\sigma_{RA}$ arcsec	$\overline{\Delta Dec}$ arcsec	$\sigma_{Dec}$ arcsec
sky survey matches	290	-0.17	0.82	-0.21	0.81
all matches	320	-0.16	0.83	-0.18	0.82

Note: each offset is measured in the sense optical–radio and PKS 0406–311 is not included.

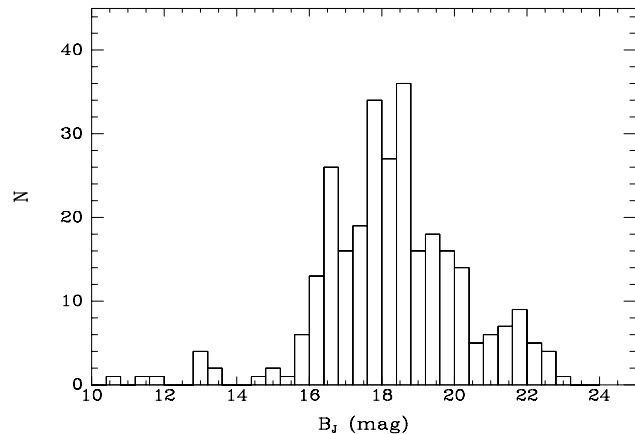
same table also shows the final results with fainter objects matched on CCD frames included.) The mean differences are small (about 0.2 arcsec) but significant (4 sigma formally) in both RA and Dec: these indicate that some residual systematic effects remain, mostly likely due to remaining second-order errors in the COSMOS astrometry. The important point is that the small dispersion in both measurements allows us to place very strong limits on the identification of our sources.

We adopted a maximum difference of  $\pm 2.5$  arcsec in RA and  $\pm 2.5$  arcsec in Dec between the radio source position and nearest optical image, corresponding to a  $3\sigma$  confidence level in each coordinate. We did not remove the small systematic mean offsets before applying these limits. The maximum total separation among the objects satisfying these criteria was 2.7 arcsec. In all cases where the matching criteria were satisfied the image parameters from the automated catalogues are given in Table 5: the optical–radio position offsets in arcsec, the morphological classification and the catalogue  $B_J$  magnitude.

The morphological classifications are based on how extended the optical images are and define the images as galaxies (g), stellar (s), or too-faint-to-classify (f). In the case of the APM data there is a further category of merged images (m) where 2 or more images are too close to separate. We intentionally do not include in Table 5 the object classifications from PKSCAT90 because there is evidence that the distinction between “galaxies” and “quasars” was not applied uniformly over the whole survey (see Drinkwater & Schmidt 1996).

The calibration accuracy of the  $B_J$  photographic magnitudes from the COSMOS catalogue is quoted as being about  $\pm 0.5$  magnitudes (H. MacGillivray, private communication). We have found that some fields lack any calibration data and some seem to be incorrect by more than one magnitude, so the catalogue magnitudes should be treated with caution. We specifically checked the calibration of any fields in which the COSMOS magnitude differed by more than 2 mag from a value published in the literature by comparison with data from adjacent COSMOS fields and corrected any large errors. A histogram of the magnitudes is given in Fig. 6.

There is a further problem of objects where 2 or 3 close optical images have been merged into a single catalogue object whose centroid position is still within our  $\pm 2.5$  arcsec matching criteria. These are easy to find because the resulting “merged” image is very extended and thus mis-classified as a galaxy. This is a problem inherent in automated catalogues for which reason the classifications should always be checked. We visually inspected all the objects classified as “galaxies” to check for merging. A total of 10 such objects were found in the matched list; they are noted in Table 5 as


**Figure 6.** Histogram of the optical  $B_J$  magnitudes of all sources identified on the photographic sky surveys.

“(merge)”. We derived corrected image parameters for these merged objects by analysing images from the Digitised Sky Survey or CCD images (at other wavelengths, see next section). If the image data was obtained from CCD data, no  $B_J$  magnitude is given for the object in the table.

One additional object was included in the matched list although its position difference was greater than the  $\pm 2.5$  arcsec limits. This was PKS 0406–311 which we identified with a galaxy 7 arcsec from the nominal radio position because the head-tail radio structure did not give an accurate position but is very indicative of this type of galaxy (see above). With this galaxy and the merged objects included, a total of 291 sources from our sample of 323 have confirmed matches to objects in the optical catalogues. This leaves a total of 32 sources with no matching image in the optical catalogues. We undertook the identification of these sources using CCD imaging at other wavelengths as described in the next section.

## 4.2 Identifications at Other Wavelengths

This section describes the methods we used to find optical counterparts for the 32 sources not matched to images listed in the optical catalogues. We first inspected all the fields visually on the optical sky survey plates. Most of the sources (25) were found to be genuine “empty fields” in the sense that no optical counterpart was visible on the survey plates. In the remaining cases (7) however a counterpart was clearly visible on the plate, but it was too faint to be included in the automated catalogue or it had been merged with a neighbouring object.

We note that six of these unmatched sources were assigned optical identifications in PKSCAT90; our new accurate positions show that these need to be revised. In three cases (PKS 1349–145, PKS 1450–338, PKS 2127–096) there is a faint matching object but it is merged with a brighter image and in the other cases there is no optical counterpart at all at the correct position (PKS 0005–262, PKS 1601–222, PKS 2056–369).

To identify the sources unmatched on the sky surveys we turned to longer wavelengths, using optical  $R$ -band,  $I$ -band, and infrared  $K_n$ -band (2.0–2.3 microns) imaging on

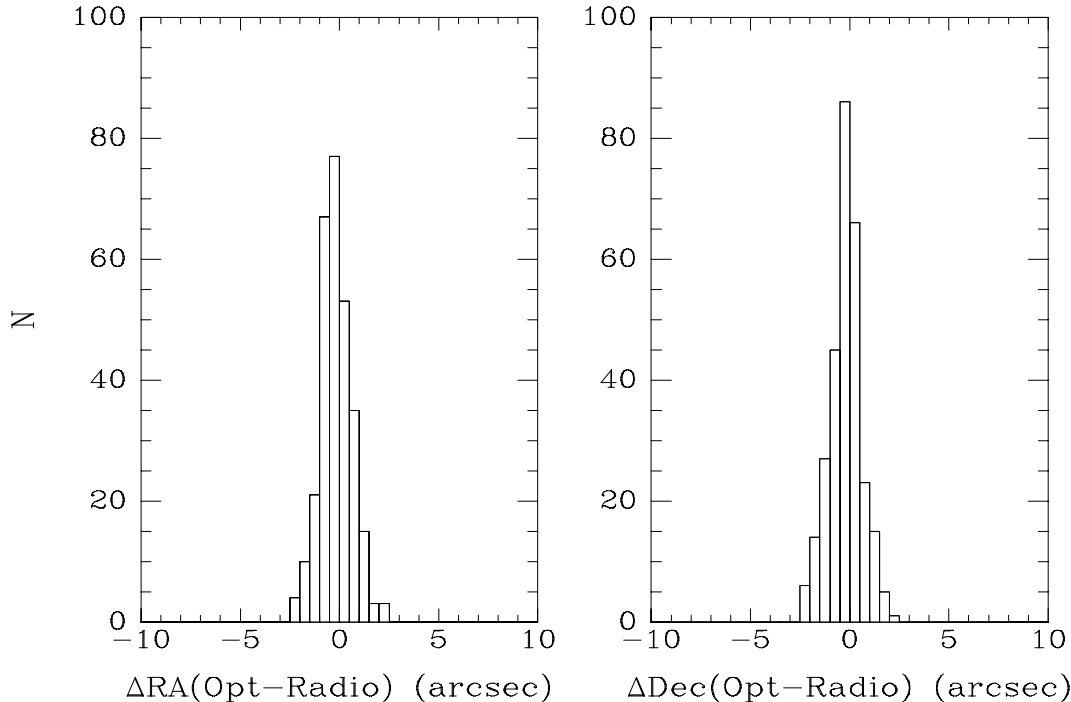


**Figure 5.** Histograms of the Position Offsets between the Radio and the Optical sources.

the 3.9m Anglo-Australian Telescope (AAT) and the Australian National University (ANU) 2.3m Telescope. These data were analysed using the IRAF<sup>‡</sup> analysis software. The observations resulted in identifications of 30 of the remaining sources including the merged objects, one of which was separated using a *B*-band image. These sources are listed in Table 5 in the same way as the sources identified from the digitised survey data, except that no *B<sub>J</sub>* magnitude is given and the position offsets are estimated from the CCD frames. The source of the identifications is indicated in the comment column as “(R)” or “(K)”. We will present a full analysis of the *R*- and *Kn*-band data in later papers.

The 2 sources we did not identify include PKS 1213–172 which lies too close to a bright star to be identified in our data but Stickel et al. (1994) report having identified it with a “*m* = 21.4 mag resolved galaxy”. The remaining source, PKS 0320+015 was not detected in a *Kn* image (approximate limit of *Kn*=18) but we anticipate identifying it when a deeper exposure is available.

We note that PKS 2149+056 which we detected in our *Kn* image was previously detected and identified as a quasar with a measured redshift by Stickel & Kühr (1993).

### 4.3 Reliability of Identifications

For the majority of the matched sources for which spectroscopic redshifts have been measured we are confident of having made the correct optical identification. For the remaining sources for which we have not yet obtained redshifts, the identifications must be made on positional coincidence alone. A very detailed analysis of the statistics of source identifications was made by Sutherland & Saunders (1992) in the context of matching IRAS sources with poor positions to the optical sky survey data. Our problem is much simpler because both our source (radio) and survey (optical) positions are accurate. Furthermore, we do not wish to include the image magnitudes in the analysis because we do not know the true distribution of optical magnitudes—a large fraction of the sources without spectroscopic confirmation are at the faint limit of the magnitude distribution.

We made an estimate of the number of “identifications” in our sample that might just be coincidences by calculating the mean surface density of images in the sky survey catalogues at the plate limit and finding how many of these would lie within the match criteria. For the 46 fields without spectroscopic confirmation we would expect 1 random matches within a radius of 3 arcsec. In fact most objects lie within 2 arcsec: at this separation we would only get 0.4 random matches. It is therefore possible that one of the identifications we claim without spectroscopic confirmation is wrong: ideally only the sources with spectroscopic identifications should be used for analysis purposes.

<sup>‡</sup> IRAF is distributed by the National Optical Astronomy Observatories, which are operated by the Association of Universities for Research in Astronomy, Inc. (AURA) under cooperative agreement with the National Science Foundation.

## 5 SPECTROSCOPIC IDENTIFICATIONS

## 5.1 Previous Results

Earlier versions of the flat-spectrum sample have been the subject of extensive campaigns of spectroscopic follow-up observations. Some two thirds of the sample were identified in the summary made by Savage et al. (1990) and we have drawn on this work for the current sample.

We carried out a very detailed literature review to find published redshifts for as much of the sample as possible. We based our search on the quasar catalogue compiled by Hewitt & Burbidge (1993) with additional material from the Véron-Cetty & Véron (1993) quasar catalogue, the Center for Astrophysics Redshift Catalog (Version of May 28, 1994; see Huchra et al. 1992), the NASA/IPAC Extragalactic Database (NED, Helou et al. 1991), and the Lyon-Meudon Extragalactic Database (LEDA). There are occasional errors in some of these large compilations, so for every redshift found in the catalogues we checked the reference cited and only accepted values for which we found a measured redshift in the original reference. We present these redshifts in Table 5 along with a code that specifies the source of the measurement. For some objects the source reference indicated that the redshift was uncertain (e.g. due to a single line or a lower limit derived from the redshift of an absorption system); in these cases the reference code is prefaced by a “-” sign. For some additional objects we found no published original reference (some were given by private communications): these are assigned a reference code of zero and we have not listed the redshift in our table.

After our critical search of the literature we accepted published redshifts for 206 sources in our sample of 323 sources. At the same time we searched for published spectra of any sources in our sample; references to these are also given in Table 5. Again, we only include those spectra we have checked in the original references.

## 5.2 New Measurements

As a result of the identifications presented in this paper we started a campaign of new spectroscopic identifications. This has resulted in 114 new spectra and 90 new redshift measurements which we present here. The journal of observations and the new redshifts are given in Table 4 and we present the spectra in Appendix C. Notes on some individual spectra are given in Section 5.3 below. Note that three sources are presented (“EXTRAS” in Table 4) that are not in our final sample. These were part of an earlier version of the sample and are included here to provide a published reference to their redshifts. Details of our observations are as follows.

Our identification of most of the “Empty Field” sources in our  $K_n$  and  $R$  band imaging enabled us to attempt spectroscopic identifications of these very faint sources. We made these observations using the AAT equipped with the RGO spectrograph (grating 250B: a resolution of  $5RA$  in the blue) and the faint object red spectrograph (FORS: a resolution of  $20RA$  in the red). We also used the AAT to observe a number of brighter objects with unconfirmed redshifts.

We made an extensive search of the AAT archive for observations of sources in our sample with no published redshifts: this provided 27 measurements.

A number of the brighter objects were observed with the

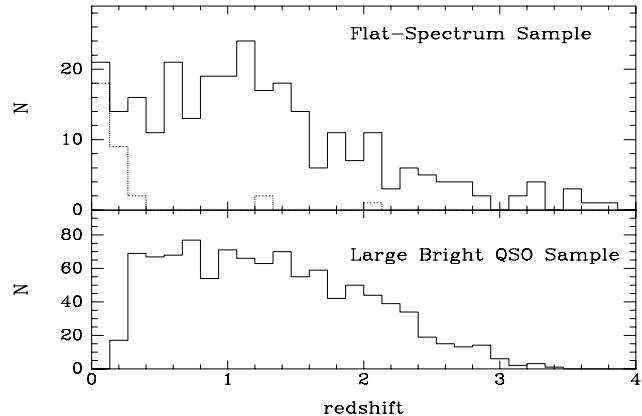


**Figure 7.** Redshift histogram for the sample: the dotted line indicates just the optically resolved sources (galaxies). The redshift histogram of a large optically selected sample, the Large Bright QSO Survey is shown in the lower panel for comparison.

ANU 2.3m Telescope using the double beam spectrograph (with a resolution of  $8RA$  in both the blue and red arms).

All these spectra were analysed with the IRAF package and any new redshifts we obtained are included in Table 5 with the reference code “121”.

Combining this new data with the published redshifts we now have confirmed redshifts for 277 or 86% of the sample and possible redshifts for a further 10. This represents a significant improvement over the last major compilation of this sample (Savage et al. 1990) when only 67% of the redshifts were measured, and not all of them published. A histogram of all the redshifts is given in Fig. 7.

## 5.3 Notes on Individual Spectra

(i) PKS 0114+074b: this is not part of the sample, but is close to PKS 0114+074 and was the source of the previously quoted redshift (see Section 3.4).

(ii) PKS 0215+015: this is not part of the sample, but was measured as part of a preliminary version of the sample and is included here for reference.

(iii) PKS 1008–017: also observed with the AAT, 1988 May 11; the combined spectrum was used.

(iv) PKS 1124–186: has weak lines but they were also observed on the AAT 1984 May 01.

(v) PKS 1336–260: also observed with the AAT, 1996 Apr 20; combined spectrum used.

(vi) PKS 1557+032: this is not part of the sample, but was measured as part of a preliminary version of the sample and is included here for reference.

(vii) PKS 1648+015: also observed with the AAT, 1995 Jun 01; combined spectrum used.

(viii) PKS 2021–330: possible broad absorption line structure near CIV.

(ix) PKS 2131–021: also observed with the ANU 2.3m Telescope, 1995 Sep 28; combined spectrum used. The redshift is based on OII and MgII in our spectra and a reported “definite” line at  $3541RA$  (Baldwin et al. 1989) which we identify with CIV.

**Table 4.** New Spectral Identifications

name	tel	date	$z_{em}$	comment	name	tel	date	$z_{em}$	comment
PKS 0036–216	AAT	1995 Sep 22	none		PKS 1143–245	ANU	1995 May 25	1.940	
PKS 0048–097	AAT	1994 Dec 02	none		PKS 1144–379	AAT	1996 Apr 21	1.047	(87)
PKS 0104–408	AAT	1984 Jun 30	none	(105)	PKS 1156–094	AAT	1996 Apr 20	none	
PKS 0114+074	AAT	1995 Sep 22	0.343	note	PKS 1228–113	AAT	1996 Apr 21	3.528	
PKS 0118–272	AAT	1994 Dec 04	>0.556		PKS 1237–101	ANU	1995 May 25	0.751	
PKS 0131–001	AAT	1994 Dec 03	0.879		PKS 1250–330	AAT	1996 Apr 20	none	
PKS 0138–097	ANU	1995 Sep 28	none	(90)	PKS 1256–229	AAT	1995 Mar 05	1.365	
PKS 0153–410	AAT	1994 Dec 04	0.226		PKS 1258–321	AAT	1988 May 10	0.017	(18)
PKS 0213–026	AAT	1994 Dec 04	1.178		PKS 1317+019	AAT	1996 Apr 21	1.232	
PKS 0216+011	AAT	1994 Dec 03	1.61		PKS 1318–263	AAT	1995 Mar 05	2.027	
PKS 0220–349	AAT	1994 Dec 04	1.49		PKS 1333–082	AAT	1988 May 10	0.023	(26)
PKS 0221+067	AAT	1986 Aug 09	0.510		PKS 1336–260	AAT	1995 Mar 05	1.51	note
PKS 0229–398	AAT	1994 Dec 04	1.646?		PKS 1340–175	AAT	1996 Apr 20	1.50?	1 line
PKS 0256+075	AAT	1994 Dec 03	0.895		PKS 1354–174	AAT	1995 Mar 06	3.137	
PKS 0301–243	AAT	1995 Sep 22	none		PKS 1359–281	AAT	1984 May 01	0.803	
PKS 0327–241	AAT	1994 Dec 04	0.888		PKS 1404–267	AAT	1988 May 10	0.022	(21)
PKS 0332–403	ANU	1995 Sep 27	none		PKS 1406–267	AAT	1996 Apr 20	2.43	
PKS 0336–017	AAT	1987 Sep 17	3.202		PKS 1430–155	AAT	1996 Apr 21	1.573	
PKS 0346–163	ANU	1995 Sep 28	none		PKS 1435–218	ANU	1996 Feb 25	1.187	
PKS 0346–279	AAT	1986 Aug 09	0.987		PKS 1445–161	AAT	1984 May 01	2.417	
PKS 0357–264	AAT	1995 Sep 22	1.47?		PKS 1450–338	AAT	1996 Apr 20	0.368	
PKS 0400–319	AAT	1994 Dec 03	1.288		PKS 1456+044	AAT	1988 May 11	0.394	
PKS 0405–331	AAT	1987 Sep 17	2.562		PKS 1511–210	AAT	1994 Apr 30	1.179	
PKS 0406–311	ANU	1995 Sep 27	0.0565		PKS 1518+045	ANU	1995 May 25	0.052	
PKS 0422+004	ANU	1995 Sep 28	none		PKS 1519–273	ANU	1996 Apr 11	none	
PKS 0423+051	AAT	1994 Dec 02	1.333		PKS 1535+004	AAT	1996 Apr 21	3.497	
PKS 0454+066	ANU	1995 Sep 28	0.4050		PKS 1615+029	AAT	1996 Apr 21	1.341	(110)
PKS 0456+060	AAT	1995 Mar 05	none		PKS 1616+063	AAT	1996 Apr 21	2.088	(3)
PKS 0459+060	AAT	1994 Dec 03	1.106		PKS 1635–035	AAT	1988 May 11	2.856?	
PKS 0502+049	AAT	1995 Mar 05	0.954		PKS 1648+015	AAT	1996 Apr 20	none	note
PKS 0508–220	ANU	1995 Nov 29	0.1715		PKS 1654–020	AAT	1996 Apr 20	2.00	
PKS 0532–378	AAT	1995 Mar 05	1.668		PKS 1706+006	AAT	1994 Sep 09	0.449	
PKS 0829+046	AAT	1994 Dec 02	none		PKS 1933–400	ANU	1995 May 25	0.965	
PKS 0837+035	AAT	1995 Mar 05	1.57		PKS 1958–179	AAT	1996 Apr 21	0.652	(10)
PKS 0859–140	AAT	1996 Apr 21	1.337	(84)	PKS 2004–447	AAT	1984 May 02	0.240	
PKS 0907–023	AAT	1995 Mar 05	0.957	(110)	PKS 2021–330	AAT	1996 Apr 21	1.471	(98) note
PKS 0912+029	AAT	1988 May 11	0.427		PKS 2022–077	AAT	1988 May 10	1.388	
PKS 0922+005	AAT	1995 Mar 05	1.717		PKS 2056–369	AAT	1995 Jul 06	none	
PKS 1008–017	ANU	1996 Apr 10	0.887	note	PKS 2058–135	AAT	1988 May 10	0.0291	(21)
PKS 1016–311	AAT	1988 May 10	0.794		PKS 2058–297	AAT	1984 May 02	1.492	
PKS 1020–103	ANU	1996 Apr 26	0.1966	(112)	PKS 2059+034	AAT	1996 Apr 21	1.012	(110)
PKS 1021–006	ANU	1996 Apr 26	2.549	(110)	PKS 2120+099	AAT	1987 Sep 17	0.932	
PKS 1036–154	AAT	1995 Mar 05	0.525		PKS 2127–096	AAT	1995 Jul 06	>0.780	>0.733
PKS 1038+064	ANU	1996 Apr 26	1.264	(84)	PKS 2128–123	AAT	1996 Apr 21	0.499	(95)
PKS 1048–313	AAT	1995 May 31	1.429		PKS 2131–021	ANU	1995 Jun 01	1.285	note
PKS 1055–243	AAT	1995 Mar 05	1.086		PKS 2143–156	ANU	1995 May 25	0.698	
PKS 1102–242	AAT	1984 May 01	1.666		PKS 2145–176	AAT	1987 Sep 17	2.130	
PKS 1106+023	AAT	1988 May 10	0.157		PKS 2215+020	AAT	1986 Aug 10	3.572	
PKS 1107–187	AAT	1995 Mar 05	0.497		PKS 2229–172	AAT	1995 Jul 06	1.780	
PKS 1110–217	AAT	1996 Apr 20	none		PKS 2233–148	AAT	1995 Jul 06	>0.609	
PKS 1115–122	AAT	1988 May 10	1.739		PKS 2252–090	AAT	1996 Jul 19	0.6064	
PKS 1118–056	AAT	1988 May 11	1.297?		PKS 2254–367	AAT	1988 May 11	0.0055	(21)
PKS 1124–186	ANU	1996 Apr 26	1.048	note	PKS 2312–319	ANU	1995 Sep 28	1.323	>1.0453
PKS 1127–145	AAT	1996 Apr 21	1.187	(107)	PKS 2329–415	AAT	1987 Sep 17	0.671	
PKS 1128–047	AAT	1984 May 01	0.266		PKS 2335–181	AAT	1987 Sep 17	1.450	
PKS 1133–172	AAT	1994 Apr 30	1.024			EXTRAS			
PKS 1136–135	ANU	1996 Apr 26	0.5566	(107)	PKS 0114+074b	AAT	1995 Sep 22	0.858	note
PKS 1142+052	AAT	1986 Apr 11	1.342	(105)	PKS 0215+015	AAT	1994 Dec 02	1.718	note
PKS 1142–225	AAT	1996 Apr 21	1.141		PKS 1557+032	AAT	1995 Mar 5	3.88	note

Notes: 1. Specific notes on individual spectra are given in Section 5.3. 2. Redshifts of any absorption systems identified in the spectra are prefaced by “>” as these give a lower limit to the source redshift. 3. Reference numbers in parentheses refer to previous published redshift estimates. 4. The final three sources observed are not in our sample but are included here in order to provide a published reference to their redshifts.

## 6 THE CATALOGUE

We present all the data we have collected on our sample in Table 5. We indicate the source of all published data in the table by a reference number; the references are listed in numerical order at the end of the paper. In all cases a minus sign in front of the reference number indicates an uncertain value. The specific reference numbers 120 and 121 refer to new data we present in this paper: 120 to accurate radio positions measured with the ATCA and 121 to all our other data including the VLA radio positions.

The columns in the table are as follows:

(i) name: the Parkes source name.  
 (ii)  $S_{2.7}$ ,  $S_{5.0}$ ,  $\alpha$ , Rf: the 2.7 and 5.0 GHz source fluxes and corresponding spectral index as published in reference Rf (see Table 1).

(iii) RA(B1950), Dec(B1950), Rc: the accurate B1950 (i.e. equinox B1950 and epoch B1950) radio source positions from reference Rc.

(iv) comment: (1) a brief description of the radio morphology if the source is resolved using the terminology of Downes et al. (1986): “P” for partially resolved sources, “Do” for double sources with no central component with the position defined by the centroid of the source, “Do+CC” for double sources with a central component or peak giving a well-defined position, “H” for a diffuse halo around a central source, and “HT” for a complex head-tail morphology. (2) comments in parentheses refer to the optical identification. In cases where there was no match to the sky catalogues but the source was identified using CCD data, these are indicated as “(B)”, “(R)”, “(I)” and “(K)” for the respective wavebands. If the CCD imaging did not identify the source, the comment “null” is made and “STR” indicates a source too near a bright star. If the source was confused with a close neighbour in the sky catalogues, but separated by a CCD image the comment “merge” is made followed by the waveband used; in some cases the Digitized Sky Survey data was used to separate the object (“DSS”).

(v)  $\Delta RA$ ,  $\Delta Dec$ ,  $\Delta r$ , cl,  $B_J$ : the position offsets (arcsec, in the sense optical–radio) of the corresponding optical image (if any), the total separation, the image classification (“g” galaxy, “s” stellar, “f” too faint to classify, “m” merged) and the apparent  $B_J$  magnitude if the counterpart was found in the sky survey data.

(vi)  $z$ , Rz, Rsp: the emission redshift of the source obtained from reference code Rz. If no emission redshift has been measured, but absorption lines have been identified these are used to place a lower limit on the source redshift indicated in the form “>0.500”. If a spectrum has been published it can be found in reference Rsp.

(vii) RA(J2000), Dec(J2000): the corresponding J2000 positions.

## 7 OVERVIEW OF THE SAMPLE

We defer a detailed analysis of the sample to other papers, but we take this opportunity to make a brief overview of the sample.

The sources with measured redshifts span the redshift range 0.05–3.78 with a median redshift of 1.07 (see Fig. 7). The redshift histogram is smooth, and broadly similar to

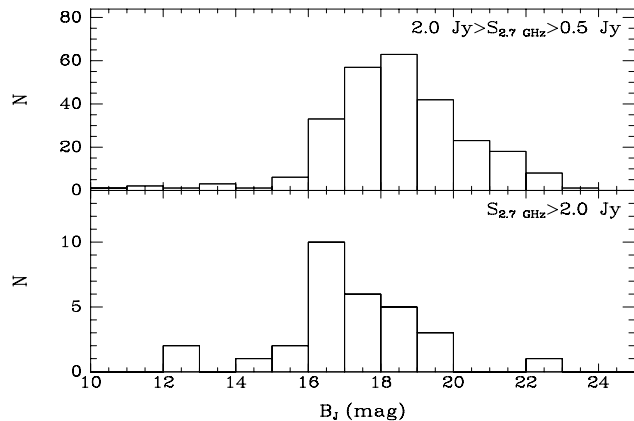


**Figure 8.** The distribution of  $B_J$  magnitudes in the sample as a function of 2.7 GHz radio fluxes.

that of optical surveys such as the Large Bright QSO Survey (LBQS; see Hewett et al. 1995, and references therein). The distribution of our sample is compared to that of the LBQS in Fig. 7. The lack of LBQS quasars in the lowest redshift bin is due to the absolute magnitude and redshift cut-off of that survey. The 2-sample Kolmogorov-Smirnov test (comparing sources with redshift  $z > 0.22$  in both samples: 235 Parkes and 1018 LBQS) gives results consistent with the two samples having the same redshift distribution at the 35% probability level. This makes the two samples ideal for comparing the properties of radio- and optically-selected quasars.

The distribution of optical  $B_J$  magnitudes of our sources (see Figs. 6 and 8) shows that despite the fact that our sample was not selected on the basis of optical magnitude, the sources occupy a restricted range of magnitudes. The majority have  $B_J = 18 \pm 3$ . The well-defined mode in the distribution of  $B_J$  magnitudes is not an artifact of the plate limit of  $B_J \approx 22.5$ ; the number of sources with  $22 > B_J > 20$  is clearly below that with  $20 > B_J > 18$ . However a small fraction of sources are clearly very faint in  $B_J$ .

In common with Browne & Wright (1985) we find that the modal  $B_J$  magnitude of our flat-spectrum sample is a function of radio flux; the most radio-bright sources have slightly brighter typical  $B_J$  magnitudes (Fig. 8). This is also shown in Fig. 9, a plot of the  $B_J$  magnitudes against the 2.7 GHz radio fluxes.

There is some suggestion from our data that the radio-to-optical ratio may be a physically meaningful parameter, as originally suggested by Schmidt (1970). In Fig. 10 we plot radio-to-optical ratios  $R$  as a function of radio luminosity, for different classes of source. A clear correlation can be seen, with the lowest radio-luminosity sources having low values of  $R$ . If, however, we exclude galaxies, the correlation disappears, and no sources remain with  $R < 100$ . The sources without redshifts have radio-to-optical ratios above those of the detected sources, which may reflect dust obscuration of the  $B_J$  emission (Webster et al. 1995).

N	name	$S_{2.7}$	$S_{5.0}$	$\alpha$	Rf	RA(B1950)	Dec(B1950)	Rc	comment	$\Delta$ RA	$\Delta$ Dec	$\Delta$ r	cl	$B_J$	z	Rz	Rsp	RA(J2000)	Dec(J2000)
1	PKS0003-066	1.46	1.58	0.13	103	0:03:40.29	-6:40:17.3	56		1.15	-0.22	1.17	s	18.47	0.347	87	87	0:06:13.89	-6:23:35.2
2	PKS0005-239	0.58	0.53	-0.15	103	0:05:27.47	-23:56:00.0	121		0.04	-0.31	0.31	s	16.61	1.407	114	108	0:08:00.37	-23:39:18.0
3	PKS0005-262	0.58	0.58	0.00	103	0:05:53.51	-26:15:53.4	121	(K)	0.39	-0.02	0.39	s	0.00	0.0	0	0	0:08:26.25	-25:59:11.5
4	PKS0008-264	0.67	0.81	0.31	103	0:08:28.89	-26:29:14.8	57		1.17	0.42	1.24	s	19.46	1.096	117	0	0:11:01.25	-26:12:33.3
5	PKS0013-005	0.89	0.79	-0.19	102	0:13:37.35	-0:31:52.5	57		-0.75	-0.21	0.78	s	19.41	1.574	105	25	0:16:11.08	-0:15:12.3
6	PKS0036-216	0.53	0.60	0.20	103	0:36:00.44	-21:36:33.1	57		0.28	-1.29	1.31	g	21.05	0.0	0	121	0:38:29.95	-21:20:03.9
7	PKS0038-020	0.61	0.79	0.42	102	0:38:24.23	-2:02:59.3	56		-0.03	-1.21	1.21	s	18.80	1.178	110	0	0:40:57.61	-1:46:32.0
8	PKS0048-097	1.44	1.92	0.47	103	0:48:09.98	-9:45:24.3	56		0.48	0.44	0.65	s	16.75	0.0	0	121	0:50:41.32	-9:29:05.2
9	PKS0048-071	0.70	0.67	-0.07	103	0:48:36.20	-7:06:20.5	57		-0.87	-1.92	2.11	f	22.06	1.974	107	108	0:51:08.20	-6:50:01.8
10	PKS0048-427	0.68	0.58	-0.26	6	0:48:49.02	-42:42:51.8	121		0.35	1.16	1.21	s	19.98	1.749	105	0	0:51:09.49	-42:26:33.0
11	PKS0056-001	1.80	1.38	-0.43	102	0:56:31.76	-0:09:18.8	56		-0.59	-0.60	0.84	s	17.79	0.717	44	4	0:59:05.51	0:06:51.8
12	PKS0104-408	0.57	0.85	0.65	6	1:04:27.58	-40:50:21.2	56		-1.59	-0.61	1.70	s	18.92	0.584	105	121	1:06:45.11	-40:34:19.5
13	PKS0106+013	1.88	2.82	0.66	102	1:06:04.52	1:19:01.1	56		0.08	0.06	0.10	s	18.82	2.094	110	4	1:08:38.77	1:35:00.4
14	PKS0108-079	1.02	0.89	-0.22	103	1:08:19.00	-7:57:37.6	57		1.11	0.15	1.12	s	18.47	1.773	112	108	1:10:50.01	-7:41:41.1
15	PKS0111+021	0.61	0.67	0.15	102	1:11:08.57	2:06:24.8	56		0.05	1.26	1.26	g	16.42	0.047	112	0	1:13:43.14	2:22:17.4
16	PKS0112-017	1.38	1.60	0.24	102	1:12:43.92	-1:42:55.0	56		-1.15	-1.06	1.57	s	17.85	1.381	4	4	1:15:17.09	-1:27:04.5
17	PKS0113-118	1.78	1.88	0.09	103	1:13:43.22	-11:52:04.5	56		-0.28	-1.85	1.87	s	19.42	0.672	91	108	1:16:12.52	-11:36:15.3
18	PKS0114+074	0.90	0.67	-0.48	-79	1:14:50.48	7:26:00.3	121	Do	-0.45	-1.50	1.57	g	22.14	0.343	121	121	1:17:27.13	7:41:47.7
19	PKS0116+082	1.50	1.11	-0.49	-79	1:16:24.24	8:14:10.0	97	P	0.00	-1.30	1.30	s	21.85	0.594	81	81	1:19:01.27	8:29:55.2
20	PKS0116-219	0.57	0.51	-0.18	103	1:16:32.40	-21:57:15.2	56		-1.20	-2.01	2.34	s	19.64	1.161	107	108	1:18:57.25	-21:41:29.9
21	PKS0118-272	0.96	1.18	0.33	103	1:18:09.53	-27:17:07.4	56		-0.03	-0.93	0.93	s	17.47	>0.556	-121	121	1:20:31.66	-27:01:24.4
22	PKS0119+041	1.83	2.01	0.15	79	1:19:21.39	4:06:44.0	56		-0.15	0.20	0.25	s	19.18	0.637	63	0	1:21:56.86	4:22:24.8
23	PKS0122-003	1.43	1.24	-0.23	102	1:22:55.18	-0:21:31.3	56		-0.39	-0.15	0.42	s	16.49	1.08	10	0	1:25:28.84	-0:05:55.9
24	PKS0130-171	0.99	0.97	-0.03	103	1:30:17.66	-17:10:11.3	120		0.24	-1.53	1.55	s	17.65	1.022	107	108	1:32:43.45	-16:54:47.8
25	PKS0130-447	0.59	0.49	-0.30	6	1:30:52.91	-44:46:05.1	120	(K)	0.05	-1.31	1.31	f	0.00	0.0	0	0	1:33:00.33	-44:30:50.9
26	PKS0131-001	0.68	0.50	-0.50	102	1:31:38.98	-0:11:35.9	55	(K)	-1.38	0.31	1.41	f	0.00	0.879	121	121	1:34:12.71	0:03:45.1
27	PKS0133-204	0.68	0.63	-0.12	103	1:33:13.59	-20:24:04.6	39		-0.81	-0.55	0.98	s	18.18	1.141	107	108	1:35:37.46	-20:08:46.1
28	PKS0135-247	1.37	1.65	0.30	103	1:35:17.12	-24:46:08.2	120		0.26	-0.96	0.99	s	18.93	0.829	107	108	1:37:38.35	-24:30:53.2
29	PKS0137+012	1.07	0.82	-0.43	102	1:37:22.87	1:16:35.4	43		-0.36	-0.07	0.37	g	19.44	0.260	44	2	1:39:57.34	1:31:45.8
30	PKS0138-097	0.71	1.19	0.84	103	1:38:56.86	-9:43:51.8	45		-0.36	-0.20	0.42	s	18.50	>0.501	-90	121	1:41:25.83	-9:28:43.7
31	PKS0142-278	0.82	0.90	0.15	103	1:42:45.01	-27:48:34.7	120		-0.84	1.35	1.59	s	17.47	1.153	107	108	1:45:03.41	-27:33:33.5
32	PKS0146+056	0.72	0.73	0.02	79	1:46:45.53	5:41:00.8	56		-0.60	0.50	0.78	s	20.67	2.345	75	0	1:49:22.37	5:55:53.7
33	PKS0150-334	0.92	0.86	-0.11	78	1:50:56.99	-33:25:10.7	56		-0.50	-0.39	0.64	s	17.38	0.610	114	108	1:53:10.13	-33:10:25.7
34	PKS0153-410	1.22	0.94	-0.42	6	1:53:31.07	-41:03:22.2	120		2.40	0.50	2.45	g	19.41	0.226	121	121	1:55:37.04	-40:48:42.3
35	PKS0202-172	1.40	1.38	-0.02	103	2:02:34.52	-17:15:39.4	56		1.48	-1.69	2.25	s	18.21	1.74	117	0	2:04:57.68	-17:01:19.7
36	PKS0213-026	0.50	0.57	0.21	102	2:13:09.87	-2:36:51.5	57	(R)	0.33	1.87	1.90	f	0.00	1.178	121	121	2:15:42.01	-2:22:56.7
37	PKS0216+011	0.50	0.64	0.40	102	2:16:32.46	1:07:13.4	56		-0.60	0.47	0.77	f	21.82	1.61	121	121	2:19:07.03	1:20:59.8
38	PKS0220-349	0.60	0.61	0.03	78	2:20:49.61	-34:55:05.2	40		-1.07	-0.13	1.08	f	21.50	1.49	121	121	2:22:56.40	-34:41:28.7
39	PKS0221+067	0.79	0.77	-0.04	79	2:21:49.96	6:45:50.4	56		-0.58	0.10	0.59	s	20.76	0.510	121	121	2:24:28.42	6:59:23.4
40	PKS0226-038	0.66	0.55	-0.30	102	2:26:21.96	-3:50:58.6	120		2.12	0.30	2.14	s	17.59	2.0660	94	84	2:28:53.09	-3:37:37.1

N	name	$S_{2.7}$	$S_{5.0}$	$\alpha$	Rf	RA(B1950)	Dec(B1950)	Rc	comment	$\Delta$ RA	$\Delta$ Dec	$\Delta$ r	cl	$B_J$	z	Rz	Rsp	RA(J2000)	Dec(J2000)
41	PKS0229-398	0.64	0.68	0.10	6	2:29:51.99	-39:49:00.2	39	(mrg R)	-0.69	0.86	1.10	m	22.28	1.646	-121	121	2:31:51.79	-39:35:47.1
42	PKS0232-042	0.84	0.62	-0.49	103	2:32:36.51	-4:15:08.9	39		0.62	-1.15	1.31	s	16.21	1.437	84	84	2:35:07.25	-4:02:04.1
43	PKS0237+040	0.73	0.77	0.09	79	2:37:14.41	4:03:29.7	56		-0.74	0.20	0.77	s	18.48	0.978	75	0	2:39:51.26	4:16:21.6
44	PKS0238-084	0.58	1.40	1.43	103	2:38:37.36	-8:28:09.0	56		-0.34	0.53	0.63	g	11.73	0.005	67	0	2:41:04.80	-8:15:20.7
45	PKS0240-217	0.97	0.82	-0.27	103	2:40:19.23	-21:45:11.6	120		0.99	1.01	1.42	g	19.05	0.314	117	108	2:42:35.80	-21:32:27.8
46	PKS0240-060	0.53	0.52	-0.03	103	2:40:43.24	-6:03:37.5	121		0.18	-0.86	0.88	s	18.20	1.800	3	0	2:43:12.46	-5:50:55.2
47	PKS0256+075	0.69	0.98	0.57	79	2:56:46.99	7:35:45.2	57		-0.44	-0.40	0.60	s	18.89	0.895	121	121	2:59:27.07	7:47:39.7
48	PKS0301-243	0.52	0.39	-0.47	103	3:01:14.22	-24:18:52.6	121	H	0.67	-0.50	0.84	s	16.43	0.0	0	121	3:03:26.50	-24:07:11.0
49	PKS0316-444	0.82	0.62	-0.45	6	3:16:13.40	-44:25:09.2	121		0.61	-2.09	2.18	g	14.87	0.076	48	0	3:17:57.68	-44:14:15.1
50	PKS0320+015	0.52	0.42	-0.35	102	3:20:34.61	1:35:12.7	121	(K null)	0.00	0.00	0.00	-	0.00	0.0	0	0	3:23:09.86	1:45:50.7
51	PKS0327-241	0.63	0.73	0.24	103	3:27:43.87	-24:07:22.9	57		-1.56	0.07	1.56	s	19.39	0.888	121	121	3:29:54.06	-23:57:08.5
52	PKS0332+078	0.74	0.81	0.15	79	3:32:12.10	7:50:16.7	56	(R)	0.13	-0.42	0.44	f	0.00	0.0	0	0	3:34:53.31	8:00:14.5
53	PKS0332-403	1.96	2.60	0.46	6	3:32:25.23	-40:18:24.0	57		0.28	-0.29	0.40	s	16.80	0.0	0	121	3:34:13.64	-40:08:25.3
54	PKS0336-017	0.58	0.46	-0.38	102	3:36:28.79	-1:43:00.4	121		-0.81	-1.09	1.36	s	20.14	3.202	121	121	3:39:00.98	-1:33:17.5
55	PKS0336-019	2.23	2.30	0.05	102	3:36:58.95	-1:56:16.9	56		-0.74	-1.01	1.25	s	18.43	0.850	110	0	3:39:30.93	-1:46:35.7
56	PKS0338-214	0.82	0.94	0.22	103	3:38:23.28	-21:29:07.9	56		0.74	-0.17	0.76	s	16.03	0.048	114	108	3:40:35.60	-21:19:31.1
57	PKS0346-163	0.54	0.55	0.03	103	3:46:21.83	-16:19:25.5	121		0.61	-0.74	0.95	s	17.41	0.0	0	121	3:48:39.27	-16:10:17.7
58	PKS0346-279	1.10	0.96	-0.22	103	3:46:34.03	-27:58:20.7	57		0.48	0.96	1.07	s	20.49	0.987	121	121	3:48:38.14	-27:49:13.2
59	PKS0348+049	0.54	0.41	-0.45	79	3:48:15.50	4:57:21.2	121	(R)	-1.37	0.93	1.66	f	0.00	0.0	0	0	3:50:54.20	5:06:21.3
60	PKS0348-120	0.50	0.54	0.12	103	3:48:49.16	-12:02:21.1	121		-1.16	-1.91	2.23	s	17.87	1.520	117	0	3:51:10.96	-11:53:22.5
61	PKS0349-278	2.89	2.21	-0.44	103	3:49:31.81	-27:53:31.5	121	H	-0.47	1.44	1.51	g	16.77	0.0662	49	0	3:51:35.77	-27:44:34.9
62	PKS0357-264	0.58	0.47	-0.34	103	3:57:28.46	-26:23:57.9	121		-0.58	-0.56	0.81	s	21.76	1.47	-121	121	3:59:33.67	-26:15:31.0
63	PKS0400-319	1.14	1.03	-0.16	78	4:00:23.61	-31:55:41.9	121		-0.66	-1.63	1.75	s	20.21	1.288	121	121	4:02:21.27	-31:47:25.8
64	PKS0402-362	1.04	1.39	0.47	6	4:02:02.60	-36:13:11.8	56		-0.01	-0.61	0.61	s	17.03	1.417	58	108	4:03:53.75	-36:05:01.8
65	PKS0403-132	3.15	3.24	0.05	103	4:03:13.98	-13:16:18.1	57		0.63	-0.17	0.65	s	16.78	0.571	117	0	4:05:34.00	-13:08:13.6
66	PKS0405-385	1.02	1.06	0.06	6	4:05:12.07	-38:34:24.7	57		-0.83	-0.16	0.84	g	19.76	1.285	98	98	4:06:59.08	-38:26:26.7
67	PKS0405-123	2.35	1.81	-0.42	103	4:05:27.46	-12:19:32.5	57		1.84	-1.24	2.22	s	14.45	0.574	93	93	4:07:48.42	-12:11:36.6
68	PKS0405-331	0.70	0.63	-0.17	78	4:05:38.55	-33:11:42.0	57		0.60	-0.03	0.61	s	19.41	2.562	121	121	4:07:33.91	-33:03:45.9
69	PKS0406-311	0.55	0.55	0.00	78	4:06:28.10	-31:08:00.0	-121	HT	-5.59	-4.52	7.19	g	15.99	0.0565	121	121	4:08:26.34	-31:00:07.2
70	PKS0406-127	0.59	0.61	0.05	103	4:06:45.33	-12:46:39.0	57		1.03	0.01	1.03	s	17.99	1.563	116	108	4:09:05.77	-12:38:48.1
71	PKS0407-170	0.55	0.41	-0.48	103	4:07:21.64	-17:03:24.1	121	(K)	0.11	-1.18	1.19	f	0.00	0.0	0	0	4:09:37.33	-16:55:35.4
72	PKS0413-210	1.79	1.36	-0.45	103	4:13:53.62	-21:03:51.1	57		-0.27	0.16	0.31	s	18.64	0.808	107	108	4:16:04.36	-20:56:27.6
73	PKS0414-189	1.18	1.31	0.17	103	4:14:23.35	-18:58:29.7	56		-0.04	0.07	0.09	s	19.35	1.536	34	108	4:16:36.54	-18:51:08.3
74	PKS0420-014	1.92	2.14	0.18	102	4:20:43.54	-1:27:28.7	121		-0.56	-1.56	1.65	s	17.38	0.914	110	109	4:23:15.80	-1:20:33.0
75	PKS0421+019	0.76	0.72	-0.09	102	4:21:32.67	1:57:32.7	56		0.37	0.25	0.45	s	17.10	2.0548	94	84	4:24:08.56	2:04:25.0
76	PKS0422+004	1.25	1.55	0.35	102	4:22:12.52	0:29:16.7	57		-0.26	-0.49	0.56	s	16.19	0.0	0	121	4:24:46.84	0:36:06.4
77	PKS0423-163	0.55	0.44	-0.36	103	4:23:37.66	-16:19:25.1	55	(K)	0.62	-0.23	0.66	f	0.00	0.0	0	0	4:25:53.56	-16:12:40.4
78	PKS0423+051	0.61	0.68	0.18	79	4:23:57.23	5:11:37.3	57		-0.29	-0.40	0.49	g	19.23	1.333	121	121	4:26:36.59	5:18:19.8
79	PKS0426-380	1.04	1.14	0.15	6	4:26:54.71	-38:02:52.1	56		1.00	-0.13	1.01	s	18.37	>1.030	-90	90	4:28:40.42	-37:56:19.5
80	PKS0430+052	3.30	3.78	0.22	-79	4:30:31.60	5:14:59.5	56		0.74	-0.60	0.95	g	12.85	0.033	66	0	4:33:11.09	5:21:15.5

N	name	$S_{2.7}$	$S_{5.0}$	$\alpha$	Rf	RA(B1950)	Dec(B1950)	Rc	comment	$\Delta$ RA	$\Delta$ Dec	$\Delta$ r	cl	$B_J$	z	Rz	Rsp	RA(J2000)	Dec(J2000)
81	PKS0434-188	1.05	1.19	0.20	103	4:34:48.97	-18:50:48.2	56		-0.46	0.06	0.46	s	18.70	2.705	107	108	4:37:01.48	-18:44:48.6
82	PKS0438-436	6.50	7.00	0.12	6	4:38:43.18	-43:38:53.1	56		-0.05	-0.21	0.22	s	19.08	2.852	52	52	4:40:17.17	-43:33:08.1
83	PKS0440-003	3.53	3.13	-0.20	102	4:40:05.29	-0:23:20.6	56		-0.31	-0.60	0.67	s	18.21	0.844	75	4	4:42:38.66	-0:17:43.4
84	PKS0445+097	0.68	0.56	-0.32	79	4:45:36.99	9:45:37.2	121		1.02	0.40	1.10	g	20.22	2.115	94	5	4:48:21.70	9:50:51.1
85	PKS0448-392	0.89	0.89	0.00	6	4:48:00.45	-39:16:15.7	39		0.51	-0.18	0.54	s	16.76	1.288	114	108	4:49:42.24	-39:11:09.4
86	PKS0451-282	2.38	2.50	0.08	103	4:51:15.13	-28:12:29.3	56		0.84	0.05	0.84	s	17.75	2.5637	8	8	4:53:14.64	-28:07:37.2
87	PKS0454+066	0.50	0.44	-0.21	-79	4:54:26.41	6:40:30.1	56		-0.91	-0.90	1.28	s	19.79	0.4050	121	121	4:57:07.71	6:45:07.3
88	PKS0454-234	1.76	2.00	0.21	103	4:54:57.29	-23:29:28.7	56		-0.11	0.55	0.56	s	18.16	1.003	87	87	4:57:03.16	-23:24:52.4
89	PKS0456+060	0.78	0.58	-0.48	79	4:56:08.15	6:03:33.9	121	(K)	-1.25	-1.26	1.78	f	0.00	0.0	0	121	4:58:48.76	6:08:04.0
90	PKS0457+024	1.63	1.47	-0.17	102	4:57:15.54	2:25:05.6	56		-1.92	1.08	2.20	s	18.24	2.382	110	4	4:59:52.04	2:29:31.1
91	PKS0458-020	1.99	1.76	-0.20	102	4:58:41.35	-2:03:33.9	57		1.15	-2.23	2.51	s	19.12	2.310	3	4	5:01:12.81	-1:59:14.3
92	PKS0459+060	0.99	0.78	-0.39	79	4:59:34.78	6:04:52.0	121		-0.16	-1.10	1.11	s	19.68	1.106	121	121	5:02:15.44	6:09:07.5
93	PKS0500+019	2.47	1.85	-0.47	102	5:00:45.18	1:58:53.8	56	(K)	-1.45	0.52	1.54	f	0.00	0.0	0	0	5:03:21.20	2:03:04.5
94	PKS0502+049	0.59	0.82	0.53	79	5:02:43.81	4:55:40.6	57		-0.31	0.10	0.32	s	18.70	0.954	121	121	5:05:23.18	4:59:42.8
95	PKS0508-220	0.90	0.68	-0.45	-7	5:08:53.20	-22:05:32.5	120		-0.38	-0.10	0.39	g	16.89	0.1715	121	121	5:11:00.50	-22:01:55.3
96	PKS0511-220	1.21	1.27	0.08	7	5:11:41.82	-22:02:41.2	56		-1.37	-0.69	1.54	g	20.24	0.0	0	108	5:13:49.11	-21:59:16.0
97	PKS0514-161	0.80	0.76	-0.08	7	5:14:01.08	-16:06:22.6	56		-1.25	-1.39	1.87	s	16.85	1.278	114	84	5:16:15.93	-16:03:07.6
98	PKS0521-365	12.50	9.23	-0.49	6	5:21:12.99	-36:30:16.0	121	Do+CC	1.09	-0.18	1.10	g	16.74	0.0552	96	96	5:22:57.99	-36:27:30.9
99	PKS0528-250	1.32	1.13	-0.25	7	5:28:05.21	-25:05:44.6	57		-0.18	-0.21	0.28	s	17.73	2.765	80	80	5:30:07.96	-25:03:29.8
100	PKS0532-378	0.70	0.59	-0.28	6	5:32:35.25	-37:49:21.8	121		-0.14	1.22	1.23	s	21.37	1.668	121	121	5:34:17.49	-37:47:25.8
101	PKS0533-120	0.80	0.64	-0.36	-7	5:33:13.75	-12:04:14.2	55		-0.77	-1.56	1.74	g	18.64	0.1573	15	0	5:35:33.31	-12:02:22.4
102	PKS0537-158	0.63	0.61	-0.05	7	5:37:17.18	-15:52:05.1	39		-1.08	-0.27	1.11	s	16.54	0.947	116	108	5:39:32.03	-15:50:30.8
103	PKS0537-441	3.84	3.80	-0.02	6	5:37:21.00	-44:06:46.8	56		0.66	1.55	1.68	s	15.45	0.893	107	108	5:38:50.28	-44:05:11.1
104	PKS0537-286	0.74	0.99	0.47	7	5:37:56.93	-28:41:28.0	56		-0.53	0.11	0.54	s	19.29	3.11	115	115	5:39:54.27	-28:39:55.9
105	PKS0622-441	0.77	0.89	0.24	6	6:22:02.68	-44:11:23.0	39	(mrgDSS)	0.00	-0.15	0.15	m	18.59	0.688	114	108	6:23:31.74	-44:13:02.4
106	PKS0629-418	0.53	0.74	0.54	6	6:29:37.72	-41:52:15.7	121		-1.11	0.21	1.13	s	18.07	1.416	38	0	6:31:12.05	-41:54:28.3
107	PKS0823+033	0.87	1.13	0.42	102	8:23:13.54	3:19:15.3	56	(mrg R)	0.02	0.86	0.86	m	0.00	0.506	90	90	8:25:50.33	3:09:24.3
108	PKS0829+046	0.62	0.70	0.20	79	8:29:10.89	4:39:50.8	57		-0.17	-0.50	0.53	s	16.03	0.0	0	121	8:31:48.87	4:29:39.0
109	PKS0837+035	0.69	0.59	-0.25	102	8:37:12.37	3:30:32.8	57		-0.73	0.60	0.95	s	20.40	1.57	121	121	8:39:49.19	3:19:53.6
110	PKS0859-140	2.93	2.29	-0.40	-7	8:59:54.95	-14:03:38.9	56		-0.52	0.30	0.60	s	16.33	1.337	121	121	9:02:16.83	-14:15:31.0
111	PKS0906+015	1.20	1.04	-0.23	102	9:06:35.19	1:33:48.0	56		0.81	-0.43	0.92	s	17.17	1.018	14	108	9:09:10.10	1:21:35.4
112	PKS0907-023	0.57	0.42	-0.50	102	9:07:13.13	-2:19:16.4	39	(mrgDSS)	0.21	0.38	0.43	m	19.11	0.957	110	121	9:09:44.95	-2:31:30.8
113	PKS0912+029	0.54	0.46	-0.26	102	9:12:01.95	2:58:27.7	121		-0.01	-0.20	0.20	s	19.56	0.427	121	121	9:14:37.92	2:45:59.0
114	PKS0921-213	0.53	0.42	-0.38	7	9:21:21.82	-21:22:52.3	121	Do+CC	-0.64	-0.32	0.72	g	16.40	0.052	59	0	9:23:38.87	-21:35:47.1
115	PKS0922+005	0.74	0.72	-0.04	102	9:22:33.76	0:32:12.2	56		-0.03	-0.05	0.06	s	17.26	1.717	121	121	9:25:07.82	0:19:13.7
116	PKS0925-203	0.81	0.70	-0.24	7	9:25:33.52	-20:21:44.7	39	Do+CC	-0.21	-0.42	0.47	s	16.35	0.348	59	108	9:27:51.79	-20:34:51.1
117	PKS1004-018	0.56	0.60	0.11	102	10:04:31.71	-1:52:30.9	56		-0.03	0.77	0.77	s	20.33	1.212	110	4	10:07:04.34	-2:07:11.3
118	PKS1008-017	0.80	0.61	-0.44	102	10:08:18.94	-1:45:31.6	121	P	-0.34	0.53	0.63	s	19.63	0.887	121	121	10:10:51.67	-2:00:19.8
119	PKS1016-311	0.62	0.65	0.08	78	10:16:12.60	-31:08:51.0	121		-0.71	0.09	0.72	s	17.58	0.794	121	121	10:18:28.77	-31:23:54.5
120	PKS1020-103	0.64	0.49	-0.43	8	10:20:04.18	-10:22:33.4	39		0.22	-0.38	0.44	s	15.07	0.1966	121	121	10:22:32.76	-10:37:44.2

N	©	name	$S_{2.7}$	$S_{5.0}$	$\alpha$	Rf	RA(B1950)	Dec(B1950)	Rc	comment	$\Delta$ RA	$\Delta$ Dec	$\Delta$ r	cl	$B_J$	z	Rz	Rsp	RA(J2000)	Dec(J2000)
121	0000	PKS1021-006	0.95	0.75	-0.38	102	10:21:56.19	-0:37:41.6	121		-0.09	0.23	0.25	s	17.90	2.549	121	121	10:24:29.58	-0:52:55.8
122	0000	PKS1032-199	1.10	1.15	0.07	70	10:32:37.37	-19:56:02.2	39		-0.45	0.15	0.47	s	18.33	2.189	107	108	10:35:02.16	-20:11:34.5
123	0000	PKS1034-293	1.33	1.51	0.21	70	10:34:55.83	-29:18:27.0	56		-0.62	0.76	0.99	s	15.94	0.312	87	108	10:37:16.08	-29:34:03.0
124	0000	PKS1036-154	0.75	0.78	0.06	70	10:36:39.48	-15:25:28.1	56		-0.54	0.42	0.69	s	21.80	0.525	121	121	10:39:06.71	-15:41:06.8
125	0000	PKS1038+064	1.74	1.40	-0.35	-79	10:38:40.88	6:25:58.3	121	(mrgDSS)	-0.15	-0.22	0.27	m	16.10	1.264	121	121	10:41:17.15	6:10:16.6
126	0000	PKS1042+071	0.50	0.50	0.00	79	10:42:19.46	7:11:25.0	121		-1.03	0.00	1.03	s	18.55	0.698	105	0	10:44:55.92	6:55:37.9
127	0000	PKS1045-188	0.94	1.11	0.27	70	10:45:40.09	-18:53:44.1	57		-1.02	0.00	1.02	s	18.42	0.595	53	0	10:48:06.61	-19:09:35.9
128	0000	PKS1048-313	0.80	0.73	-0.15	78	10:48:43.38	-31:22:18.5	121		-0.32	-0.15	0.35	s	18.49	1.429	121	121	10:51:04.80	-31:38:14.4
129	0000	PKS1055-243	0.77	0.61	-0.38	70	10:55:29.94	-24:17:44.6	56		-0.66	-0.02	0.66	s	19.90	1.086	121	121	10:57:55.41	-24:33:49.0
130	0000	PKS1055+018	3.02	3.07	0.03	102	10:55:55.32	1:50:03.5	56		0.04	0.27	0.27	s	18.47	0.888	110	4	10:58:29.61	1:33:58.7
131	0000	PKS1101-325	0.93	0.73	-0.39	78	11:01:08.51	-32:35:06.2	121	Do+CC	-0.99	1.53	1.82	s	16.45	0.3554	47	108	11:03:31.57	-32:51:17.0
132	0000	PKS1102-242	0.50	0.57	0.21	70	11:02:19.82	-24:15:13.6	39		-0.11	-0.15	0.18	s	20.61	1.666	121	121	11:04:46.18	-24:31:25.7
133	0000	PKS1106+023	0.64	0.50	-0.40	102	11:06:11.19	2:18:56.2	39	Do	0.58	-0.64	0.87	g	18.01	0.157	121	121	11:08:45.52	2:02:40.2
134	0000	PKS1107-187	0.65	0.50	-0.43	70	11:07:31.75	-18:42:31.8	120	(K)	-1.07	1.18	1.59	f	0.00	0.497	121	121	11:10:00.45	-18:58:49.2
135	0000	PKS1110-217	0.94	0.76	-0.34	70	11:10:21.67	-21:42:08.7	39	(I)	1.09	0.19	1.11	f	0.00	0.0	0	121	11:12:49.81	-21:58:28.8
136	0000	PKS1115-122	0.67	0.63	-0.10	8	11:15:46.13	-12:16:29.5	121		-0.45	-1.67	1.73	s	18.15	1.739	121	121	11:18:17.14	-12:32:54.2
137	0000	PKS1118-056	0.66	0.57	-0.24	8	11:18:52.51	-5:37:29.1	121		-0.60	-0.31	0.67	s	18.99	1.297	-121	121	11:21:25.10	-5:53:56.2
138	0000	PKS1124-186	0.61	0.84	0.52	70	11:24:34.02	-18:40:46.4	57		-0.82	-0.06	0.82	s	18.65	1.048	121	121	11:27:04.39	-18:57:17.6
139	0000	PKS1127-145	5.97	5.46	-0.14	8	11:27:35.67	-14:32:54.4	56		0.72	-0.01	0.72	s	16.95	1.187	121	121	11:30:07.05	-14:49:27.5
140	0000	PKS1128-047	0.74	0.90	0.32	8	11:28:57.50	-4:43:46.1	56		-2.35	0.65	2.43	f	21.41	0.266	121	121	11:31:30.52	-5:00:19.9
141	0000	PKS1133-172	0.65	0.52	-0.36	70	11:33:31.60	-17:16:36.6	121		0.12	-1.89	1.89	f	22.43	1.024	121	121	11:36:03.05	-17:33:12.9
142	0000	PKS1136-135	2.76	2.22	-0.35	8	11:36:38.43	-13:34:06.0	121	Do	1.00	0.86	1.31	s	16.30	0.5566	121	121	11:39:10.62	-13:50:43.7
143	0000	PKS1142+052	0.60	0.46	-0.43	79	11:42:47.16	5:12:06.7	121		-0.88	-0.60	1.06	s	19.79	1.342	105	121	11:45:21.33	4:55:26.9
144	0000	PKS1142-225	0.54	0.63	0.25	70	11:42:50.23	-22:33:51.8	39	(mrg R)	0.80	1.42	1.63	f	0.00	1.141	121	121	11:45:22.05	-22:50:31.8
145	0000	PKS1143-245	1.32	1.18	-0.18	70	11:43:36.37	-24:30:52.9	56		-0.08	0.54	0.54	s	17.66	1.940	121	121	11:46:08.10	-24:47:33.1
146	0000	PKS1144-379	1.07	2.22	1.18	6	11:44:30.87	-37:55:30.6	56		0.19	1.25	1.27	s	18.43	1.047	121	121	11:47:01.38	-38:12:11.1
147	0000	PKS1145-071	1.09	1.21	0.17	8	11:45:18.29	-7:08:00.7	121	(mrgDSS)	1.44	-0.91	1.70	m	19.03	1.342	107	108	11:47:51.55	-7:24:41.3
148	0000	PKS1148-001	2.56	1.95	-0.44	102	11:48:10.13	-0:07:13.2	57		-0.11	-0.82	0.83	s	17.13	1.9803	94	119	11:50:43.87	-0:23:54.4
149	0000	PKS1148-171	0.60	0.50	-0.30	70	11:48:30.38	-17:07:18.7	121		0.21	-2.35	2.36	s	17.91	1.751	116	108	11:51:03.21	-17:24:00.0
150	0000	PKS1156-221	0.71	0.78	0.15	70	11:56:37.79	-22:11:54.9	57		-1.34	-0.04	1.35	s	18.63	0.565	116	108	11:59:11.29	-22:28:37.2
151	0000	PKS1156-094	0.75	0.66	-0.21	8	11:56:39.06	-9:24:10.0	121		-0.85	0.44	0.96	f	22.57	0.0	0	121	11:59:12.71	-9:40:52.2
152	0000	PKS1200-051	0.50	0.46	-0.14	8	12:00:00.44	-5:11:20.6	121		-0.43	0.53	0.68	s	16.42	0.381	116	108	12:02:34.23	-5:28:02.8
153	0000	PKS1202-262	1.34	0.99	-0.49	70	12:02:58.82	-26:17:22.6	39	Do	-0.23	0.14	0.27	s	19.76	0.789	107	108	12:05:33.19	-26:34:04.8
154	0000	PKS1206-399	0.59	0.53	-0.17	6	12:06:59.46	-39:59:31.3	39		-0.67	-0.18	0.69	s	17.20	0.966	36	108	12:09:35.25	-40:16:13.1
155	0000	PKS1213-172	1.33	1.28	-0.06	70	12:13:11.67	-17:15:05.3	56	(K STR)	0.00	0.00	0.00	-	0.00	0.0	0	0	12:15:46.75	-17:31:45.6
156	0000	PKS1218-024	0.54	0.47	-0.23	102	12:18:49.90	-2:25:12.0	121	H	0.14	-0.11	0.18	s	20.25	0.665	105	0	12:21:23.92	-2:41:50.4
157	0000	PKS1222+037	0.81	0.86	0.10	102	12:22:19.10	3:47:27.1	56		-0.17	0.00	0.17	s	19.28	0.957	110	4	12:24:52.42	3:30:50.2
158	0000	PKS1226+023	43.40	40.00	-0.13	102	12:26:33.25	2:19:43.3	56		1.41	-0.41	1.47	s	12.93	0.158	2	2	12:29:06.70	2:03:08.5
159	0000	PKS1228-113	0.55	0.46	-0.29	8	12:28:20.06	-11:22:36.0	121		-0.31	0.45	0.54	f	22.01	3.528	121	121	12:30:55.57	-11:39:09.9
160	0000	PKS1229-021	1.33	1.05	-0.38	102	12:29:25.88	-2:07:32.1	121	Do+CC	1.48	-1.49	2.10	s	16.62	1.045	30	108	12:31:59.99	-2:24:05.4

N	name	$S_{2.7}$	$S_{5.0}$	$\alpha$	Rf	RA(B1950)	Dec(B1950)	Rc	comment	$\Delta$ RA	$\Delta$ Dec	$\Delta$ r	cl	$B_J$	z	Rz	Rsp	RA(J2000)	Dec(J2000)
161	PKS1236+077	0.59	0.67	0.21	79	12:36:52.31	7:46:45.4	56		-0.46	-0.80	0.92	s	19.14	0.40	105	108	12:39:24.58	7:30:17.1
162	PKS1237-101	1.35	1.13	-0.29	8	12:37:07.29	-10:07:00.7	57		-0.47	0.34	0.58	s	17.46	0.751	121	121	12:39:43.07	-10:23:28.9
163	PKS1243-072	0.79	1.11	0.55	8	12:43:28.79	-7:14:23.5	57		0.07	0.30	0.31	s	17.64	1.286	107	108	12:46:04.23	-7:30:46.7
164	PKS1244-255	1.34	1.55	0.24	70	12:44:06.71	-25:31:26.7	57		-0.80	-0.12	0.81	s	16.17	0.638	107	108	12:46:46.79	-25:47:49.4
165	PKS1250-330	0.52	0.49	-0.10	78	12:50:14.95	-33:03:41.9	121	P	-0.99	-0.03	0.99	s	21.42	0.0	0	121	12:52:58.47	-33:19:59.0
166	PKS1253-055	12.00	13.00	0.13	8	12:53:35.84	-5:31:08.0	56		-0.32	-0.07	0.33	s	17.67	0.540	13	0	12:56:11.17	-5:47:21.7
167	PKS1254-333	0.72	0.54	-0.47	78	12:54:36.28	-33:18:33.6	120	Do	-0.62	2.21	2.29	s	17.05	0.190	107	108	12:57:20.71	-33:34:46.3
168	PKS1255-316	1.49	1.68	0.19	78	12:55:15.18	-31:39:05.0	56		0.01	-0.87	0.87	s	18.49	1.924	38	0	12:57:59.07	-31:55:17.0
169	PKS1256-220	0.65	0.79	0.32	70	12:56:13.94	-22:03:20.4	57		0.15	-0.76	0.78	s	19.60	1.306	20	20	12:58:54.48	-22:19:31.3
170	PKS1256-229	0.50	0.54	0.12	70	12:56:27.60	-22:54:27.7	121		1.51	0.28	1.54	s	16.72	1.365	121	121	12:59:08.45	-23:10:38.4
171	PKS1258-321	0.92	0.79	-0.25	78	12:58:16.17	-32:10:20.6	120	H	0.15	-1.37	1.38	g	13.11	0.017	18	121	13:01:00.80	-32:26:29.3
172	PKS1302-102	0.89	1.00	0.19	8	13:02:55.85	-10:17:16.5	56		-0.08	0.19	0.21	s	15.71	0.286	76	0	13:05:33.01	-10:33:19.7
173	PKS1313-333	1.00	1.32	0.45	78	13:13:20.05	-33:23:09.7	56		0.58	1.16	1.29	s	16.81	1.21	37	0	13:16:07.99	-33:38:59.3
174	PKS1317+019	0.55	0.63	0.22	102	13:17:53.73	1:56:19.7	121		0.66	0.27	0.71	s	20.81	1.232	121	121	13:20:26.78	1:40:36.7
175	PKS1318-263	0.65	0.64	-0.03	70	13:18:28.86	-26:20:28.7	121		1.05	0.24	1.08	s	20.37	2.027	121	121	13:21:13.99	-26:36:10.9
176	PKS1327-311	0.52	0.56	0.12	78	13:27:29.98	-31:07:30.8	121		0.29	-1.05	1.09	s	18.46	1.335	107	108	13:30:19.09	-31:22:58.7
177	PKS1330+022	1.91	1.47	-0.42	102	13:30:20.46	2:16:08.8	121	Do+CC	0.37	1.02	1.08	g	19.40	0.2159	65	0	13:32:53.25	2:00:45.6
178	PKS1333-082	0.50	0.59	0.27	8	13:33:30.54	-8:14:34.4	121		-0.24	0.71	0.75	g	13.55	0.023	26	121	13:36:08.26	-8:29:52.1
179	PKS1334-127	2.01	2.18	0.13	8	13:34:59.80	-12:42:09.7	57		1.18	0.78	1.41	s	15.70	0.5390	89	89	13:37:39.77	-12:57:24.8
180	PKS1336-260	0.71	0.77	0.13	70	13:36:32.48	-26:05:18.2	121		0.35	-0.30	0.46	s	20.13	1.51	121	121	13:39:19.88	-26:20:30.5
181	PKS1340-175	0.76	0.56	-0.50	70	13:40:54.45	-17:32:51.7	121	(K)	1.55	1.33	2.04	f	0.00	1.50	-121	121	13:43:37.40	-17:47:55.9
182	PKS1349-145	1.04	0.93	-0.18	8	13:49:10.75	-14:34:27.0	57	(mrg K)	2.15	-1.03	2.38	f	0.00	0.0	0	0	13:51:52.65	-14:49:15.0
183	PKS1351-018	0.98	0.94	-0.07	102	13:51:32.03	-1:51:20.1	121		-0.98	-1.11	1.48	s	21.30	3.709	25	25	13:54:06.89	-2:06:03.3
184	PKS1352-104	0.79	0.98	0.35	8	13:52:06.85	-10:26:21.1	121	Do+CC	-1.34	-0.02	1.34	s	17.60	0.332	10	108	13:54:46.54	-10:41:03.1
185	PKS1353-341	0.64	0.67	0.07	78	13:53:09.82	-34:06:31.3	57		0.78	0.78	1.10	g	18.56	0.223	105	0	13:56:05.39	-34:21:11.0
186	PKS1354-174	1.28	0.97	-0.45	70	13:54:22.05	-17:29:24.7	57		-0.82	-2.20	2.35	s	17.85	3.137	121	121	13:57:06.08	-17:44:01.9
187	PKS1359-281	0.82	0.67	-0.33	70	13:59:10.69	-28:07:59.7	121		-1.58	2.00	2.55	s	18.71	0.803	121	121	14:02:02.50	-28:22:26.5
188	PKS1402-012	0.71	0.81	0.21	102	14:02:11.29	-1:16:01.8	56		0.15	-0.75	0.77	s	16.75	2.5216	94	5	14:04:45.89	-1:30:22.1
189	PKS1402+044	0.58	0.71	0.33	79	14:02:29.97	4:29:55.1	57		0.45	0.80	0.92	s	21.29	3.2109	94	108	14:05:01.11	4:15:35.5
190	PKS1403-085	0.71	0.58	-0.33	8	14:03:21.67	-8:33:49.7	121		0.13	1.11	1.11	s	18.60	1.758	107	108	14:06:00.72	-8:48:07.3
191	PKS1404-267	0.50	0.40	-0.36	70	14:04:38.30	-26:46:50.6	121		0.69	-0.21	0.72	g	13.56	0.022	121	121	14:07:29.79	-27:01:05.1
192	PKS1404-342	0.67	0.62	-0.13	78	14:04:57.20	-34:17:14.2	121		-0.52	-0.20	0.56	s	17.66	1.122	105	0	14:07:54.95	-34:31:27.9
193	PKS1406-076	0.96	1.05	0.15	8	14:06:17.90	-7:38:15.9	57		1.49	0.39	1.54	s	20.30	1.494	107	108	14:08:56.48	-7:52:26.8
194	PKS1406-267	0.57	0.90	0.74	70	14:06:58.43	-26:43:27.2	39		-0.72	-2.21	2.33	s	21.75	2.43	121	121	14:09:50.17	-26:57:36.3
195	PKS1411+094	0.60	0.45	-0.47	-79	14:11:32.40	9:29:03.7	121	Do	0.85	-1.40	1.64	g	19.73	0.162	105	0	14:14:00.13	9:15:05.1
196	PKS1417-192	1.10	0.83	-0.46	70	14:17:02.63	-19:14:40.9	121	Do+CC	-0.80	0.76	1.10	g	17.82	0.1195	11	0	14:19:49.73	-19:28:25.9
197	PKS1425-274	0.55	0.60	0.14	70	14:25:33.56	-27:28:29.0	121		0.48	0.29	0.56	s	18.14	1.082	107	108	14:28:28.22	-27:41:52.1
198	PKS1430-178	1.00	0.93	-0.12	70	14:30:10.65	-17:48:24.3	56		-1.29	1.82	2.23	s	17.82	2.326	107	108	14:32:57.69	-18:01:35.3
199	PKS1430-155	0.55	0.66	0.30	70	14:30:36.13	-15:35:34.8	57	(K)	-0.81	-1.67	1.86	f	0.00	1.573	121	121	14:33:21.46	-15:48:44.7
200	PKS1435-218	0.79	0.81	0.04	70	14:35:18.66	-21:51:57.9	57		-0.29	-1.23	1.27	s	17.41	1.187	121	121	14:38:09.47	-22:04:54.9

© 0000 RAS, MNRAS 000, 000-000	name	$S_{2.7}$	$S_{5.0}$	$\alpha$	Rf	RA(B1950)	Dec(B1950)	Rc	comment	$\Delta$ RA	$\Delta$ Dec	$\Delta$ r	cl	$B_J$	z	Rz	Rsp	RA(J2000)	Dec(J2000)
201	PKS1437-153	0.72	0.64	-0.19	70	14:37:11.35	-15:18:58.8	57		-1.24	-0.02	1.24	s	19.87	0.0	0	0	14:39:56.88	-15:31:50.6
202	PKS1438-347	0.50	0.45	-0.17	78	14:38:20.36	-34:43:57.5	121		-2.30	-0.14	2.30	s	17.58	1.159	37	0	14:41:24.01	-34:56:45.8
203	PKS1443-162	0.78	0.65	-0.30	70	14:43:06.68	-16:16:26.7	57		-0.70	0.04	0.70	s	20.53	0.0	0	0	14:45:53.37	-16:29:01.7
204	PKS1445-161	1.06	0.80	-0.46	70	14:45:28.34	-16:07:56.5	120		-0.68	0.49	0.84	s	20.40	2.417	121	121	14:48:15.06	-16:20:24.7
205	PKS1450-338	0.72	0.54	-0.47	78	14:50:58.10	-33:48:46.0	121	(mrg K)	-1.01	0.07	1.01	f	0.00	0.368	121	121	14:54:02.59	-34:00:57.6
206	PKS1454-060	0.83	0.62	-0.47	8	14:54:02.68	-6:05:39.1	121		-1.84	-1.68	2.49	s	18.27	1.249	12	0	14:56:41.48	-6:17:42.0
207	PKS1456+044	0.68	0.72	0.09	-79	14:56:29.16	4:28:09.8	121	H	-0.01	-0.10	0.10	s	20.15	0.394	121	121	14:58:59.36	4:16:14.2
208	PKS1504-166	2.30	1.96	-0.26	-7	15:04:16.42	-16:40:59.3	56	(mrgDSS)	-0.04	-0.70	0.70	m	19.05	0.876	34	0	15:07:04.79	-16:52:30.3
209	PKS1508-055	2.90	2.33	-0.36	-7	15:08:14.98	-5:31:49.0	56		0.51	0.40	0.65	s	17.12	1.185	107	108	15:10:53.60	-5:43:07.5
210	PKS1509+022	0.69	0.54	-0.40	102	15:09:43.83	2:14:30.3	121	H	-1.06	1.30	1.68	g	19.83	0.219	69	108	15:12:15.75	2:03:16.4
211	PKS1510-089	2.80	3.25	0.24	-7	15:10:08.90	-8:54:47.6	56		-0.56	0.10	0.57	s	16.21	0.362	107	108	15:12:50.53	-9:05:59.9
212	PKS1511-100	0.56	0.70	0.36	7	15:11:02.25	-10:00:51.0	57		-0.94	-0.36	1.01	s	17.61	1.513	107	108	15:13:44.89	-10:12:00.4
213	PKS1511-210	0.55	0.77	0.55	7	15:11:03.95	-21:03:48.4	57		0.62	-0.58	0.84	s	21.88	1.179	121	121	15:13:56.98	-21:14:57.5
214	PKS1514-241	2.00	1.94	-0.05	-7	15:14:45.28	-24:11:22.6	56		-1.34	0.33	1.38	g	16.44	0.0486	51	108	15:17:41.82	-24:22:19.5
215	PKS1518+045	0.50	0.37	-0.49	-79	15:18:52.71	4:31:14.2	121	H	0.31	-0.20	0.37	g	12.82	0.052	121	121	15:21:22.52	4:20:30.4
216	PKS1519-273	1.99	2.28	0.22	7	15:19:37.24	-27:19:30.2	121		-0.22	-1.21	1.23	s	18.02	0.0	0	121	15:22:37.67	-27:30:10.8
217	PKS1532+016	1.08	0.94	-0.23	102	15:32:20.16	1:41:01.7	121		0.42	0.53	0.67	s	19.04	1.435	105	4	15:34:52.44	1:31:04.2
218	PKS1535+004	1.01	0.87	-0.24	102	15:35:42.56	0:28:50.8	57	(K)	-0.30	0.00	0.30	f	0.00	3.497	121	121	15:38:15.96	0:19:05.2
219	PKS1542+042	0.53	0.47	-0.19	79	15:42:29.69	4:17:07.6	121		0.90	0.20	0.93	s	18.59	2.184	107	108	15:44:59.39	4:07:46.3
220	PKS1546+027	1.27	1.42	0.18	102	15:46:58.29	2:46:06.1	56		0.11	0.70	0.71	s	18.54	0.415	110	4	15:49:29.43	2:37:01.1
221	PKS1548+056	1.83	2.18	0.28	79	15:48:06.93	5:36:11.3	56		-0.01	-0.20	0.20	s	18.45	1.422	105	0	15:50:35.26	5:27:10.4
222	PKS1550-269	1.35	1.14	-0.27	7	15:50:59.64	-26:55:50.0	97	P	2.21	-1.31	2.56	s	19.44	2.145	38	0	15:54:02.34	-27:04:39.3
223	PKS1555+001	2.01	2.29	0.21	102	15:55:17.69	0:06:43.5	57		-0.95	-0.48	1.06	f	22.12	1.77	3	0	15:57:51.43	-0:01:50.5
224	PKS1555-140	0.73	0.83	0.21	7	15:55:33.72	-14:01:26.4	50	(mrgDSS)	0.00	0.28	0.28	m	16.99	0.097	59	108	15:58:21.92	-14:09:59.0
225	PKS1556-245	0.69	0.54	-0.40	7	15:56:41.20	-24:34:11.0	60		-1.75	0.04	1.75	s	17.79	2.8179	94	5	15:59:41.40	-24:42:39.0
226	PKS1601-222	0.57	0.44	-0.42	7	16:01:03.96	-22:15:30.2	121		-2.34	-1.40	2.73	s	20.95	0.0	0	0	16:04:01.65	-22:23:41.7
227	PKS1602-001	0.53	0.42	-0.38	102	16:02:22.11	-0:11:00.6	121	Do+CC	-0.15	0.24	0.28	s	17.71	1.6241	94	119	16:04:56.14	-0:19:07.8
228	PKS1614+051	0.67	0.85	0.39	79	16:14:09.08	5:06:54.4	57		-0.10	-0.50	0.51	s	21.07	3.2167	94	5	16:16:37.55	4:59:32.7
229	PKS1615+029	0.74	0.66	-0.19	102	16:15:19.11	2:54:00.1	57		-1.09	1.10	1.55	s	18.20	1.341	121	121	16:17:49.91	2:46:43.0
230	PKS1616+063	0.93	0.89	-0.07	79	16:16:36.54	6:20:14.3	56		-0.45	-0.30	0.54	s	19.63	2.088	121	121	16:19:03.69	6:13:02.2
231	PKS1635-035	0.51	0.48	-0.10	102	16:35:41.56	-3:34:10.0	121		-1.22	0.47	1.31	s	21.78	2.856	-121	121	16:38:19.29	-3:40:05.0
232	PKS1648+015	0.72	0.69	-0.07	102	16:48:31.58	1:34:25.7	56		0.71	-0.37	0.80	f	22.69	0.0	0	121	16:51:03.66	1:29:23.5
233	PKS1649-062	0.70	0.63	-0.17	7	16:49:00.30	-6:13:16.0	121	Do	-1.40	0.79	1.61	g	23.03	0.0	0	0	16:51:41.08	-6:18:15.9
234	PKS1654-020	0.64	0.51	-0.37	102	16:54:19.98	-2:02:12.0	121	(K)	0.17	0.06	0.18	f	0.00	2.00	121	121	16:56:56.09	-2:06:49.8
235	PKS1655+077	1.26	1.60	0.39	79	16:55:43.95	7:45:59.8	57		0.40	-0.20	0.44	s	21.66	0.621	107	108	16:58:09.00	7:41:27.6
236	PKS1656+053	1.60	2.10	0.44	79	16:56:05.62	5:19:47.0	121		-0.02	-0.30	0.30	s	17.11	0.8873	84	85	16:58:33.44	5:15:16.4
237	PKS1705+018	0.53	0.58	0.15	102	17:05:02.74	1:52:38.4	121		-0.33	-0.91	0.97	s	18.49	2.5765	94	5	17:07:34.43	1:48:45.8
238	PKS1706+006	0.50	0.38	-0.45	102	17:06:11.54	0:38:57.1	121		-0.23	0.22	0.32	f	22.80	0.449	121	121	17:08:44.62	0:35:09.4
239	PKS1725+044	0.78	1.21	0.71	79	17:25:56.34	4:29:27.9	56	(mrg K)	-0.52	0.09	0.53	m	18.20	0.296	107	108	17:28:24.95	4:27:04.9
240	PKS1732+094	1.08	0.82	-0.45	79	17:32:35.66	9:28:52.6	57	(K)	0.04	0.63	0.63	f	0.00	0.0	0	0	17:34:58.38	9:26:58.2

The Parkes Half-Jansky Flat-Spectrum Sample

N	name	$S_{2.7}$	$S_{5.0}$	$\alpha$	Rf	RA(B1950)	Dec(B1950)	Rc	comment	$\Delta$ RA	$\Delta$ Dec	$\Delta$ r	cl	$B_J$	z	Rz	Rsp	RA(J2000)	Dec(J2000)
241	PKS1933-400	1.20	1.44	0.30	6	19:33:51.12	-40:04:46.8	56		0.41	-1.28	1.34	s	17.73	0.965	121	121	19:37:16.21	-39:58:00.8
242	PKS1953-325	0.51	0.63	0.34	78	19:53:48.42	-32:33:49.9	57		0.36	1.71	1.74	s	19.94	1.242	37	108	19:56:59.49	-32:25:46.2
243	PKS1954-388	2.00	2.00	0.00	6	19:54:39.06	-38:53:13.3	56		-0.54	0.20	0.58	s	17.82	0.626	107	108	19:57:59.83	-38:45:06.1
244	PKS1958-179	1.11	1.17	0.09	7	19:58:04.61	-17:57:16.9	56		0.30	-0.02	0.30	s	17.05	0.652	121	121	20:00:57.09	-17:48:57.5
245	PKS2000-330	0.71	1.20	0.85	78	20:00:13.02	-33:00:12.5	56	(mrgDSS)	0.13	0.03	0.13	m	19.56	3.7832	94	5	20:03:24.12	-32:51:44.4
246	PKS2002-185	0.64	0.48	-0.47	7	20:02:24.43	-18:30:39.0	121		-0.10	-0.45	0.46	s	17.44	0.859	107	108	20:05:17.32	-18:22:03.3
247	PKS2004-447	0.81	0.65	-0.36	6	20:04:25.13	-44:43:28.4	39		-0.83	0.36	0.90	s	18.09	0.240	121	121	20:07:55.18	-44:34:44.0
248	PKS2008-159	0.74	1.35	0.98	7	20:08:25.91	-15:55:38.3	56		0.76	0.26	0.80	s	15.95	1.178	107	108	20:11:15.70	-15:46:40.3
249	PKS2021-330	0.79	0.90	0.21	78	20:21:26.60	-33:03:22.0	121		-0.45	0.72	0.84	s	17.60	1.471	121	121	20:24:35.56	-32:53:36.3
250	PKS2022-077	1.12	0.89	-0.37	-7	20:22:59.59	-7:45:42.4	121		-0.20	-0.86	0.89	s	18.47	1.388	121	121	20:25:40.65	-7:35:52.0
251	PKS2037-253	0.93	1.17	0.37	7	20:37:10.76	-25:18:26.4	56		0.06	-0.66	0.66	s	17.80	1.574	107	108	20:40:08.77	-25:07:46.6
252	PKS2044-168	0.77	0.80	0.06	7	20:44:30.83	-16:50:09.5	121	Do+CC	0.15	-1.04	1.05	s	17.49	1.937	106	106	20:47:19.67	-16:39:05.6
253	PKS2047+098	0.71	0.85	0.29	79	20:47:20.78	9:52:02.0	56	(K)	-0.13	2.01	2.01	f	0.00	0.0	0	0	20:49:45.86	10:03:14.4
254	PKS2053-044	0.55	0.42	-0.44	7	20:53:12.76	-4:28:18.2	121		-0.61	-0.85	1.04	s	19.05	1.177	107	108	20:55:50.24	-4:16:46.6
255	PKS2056-369	0.51	0.39	-0.44	6	20:56:32.12	-36:57:37.5	121	(K)	0.72	0.00	0.72	f	0.00	0.0	0	121	20:59:41.62	-36:45:54.5
256	PKS2058-297	0.65	0.87	0.47	7	20:58:00.91	-29:45:15.0	56		-0.91	-0.35	0.98	s	16.21	1.492	121	121	21:01:01.65	-29:33:27.7
257	PKS2058-135	0.60	0.52	-0.23	-7	20:58:59.35	-13:30:37.1	121		1.84	-0.60	1.94	g	10.60	0.0291	121	121	21:01:44.38	-13:18:47.2
258	PKS2059+034	0.59	0.75	0.39	102	20:59:08.01	3:29:41.5	56		-1.03	-0.20	1.05	s	17.64	1.012	121	121	21:01:38.83	3:41:31.4
259	PKS2106-413	2.11	2.28	0.13	6	21:06:19.39	-41:22:33.4	56		-0.92	-1.59	1.83	s	19.50	1.055	105	0	21:09:33.18	-41:10:20.4
260	PKS2120+099	0.65	0.50	-0.43	-79	21:20:47.07	9:55:02.2	121		0.02	-0.10	0.10	s	20.16	0.932	121	121	21:23:13.34	10:07:55.6
261	PKS2121+053	1.62	3.16	1.08	79	21:21:14.80	5:22:27.5	56		-0.63	0.20	0.66	s	18.31	1.941	84	84	21:23:44.51	5:35:22.3
262	PKS2126-158	1.17	1.24	0.09	7	21:26:26.78	-15:51:50.4	56		0.22	-0.79	0.82	s	16.60	3.2663	94	68	21:29:12.18	-15:38:41.0
263	PKS2127-096	0.51	0.45	-0.20	7	21:27:38.40	-9:40:49.2	121	(mrg B)	1.46	-0.57	1.57	f	0.00	>0.780	-121	121	21:30:19.08	-9:27:36.7
264	PKS2128-123	1.90	2.00	0.08	-7	21:28:52.67	-12:20:20.6	56		0.01	-1.88	1.88	s	15.97	0.499	121	121	21:31:35.25	-12:07:04.8
265	PKS2131-021	1.91	1.99	0.07	102	21:31:35.13	-2:06:40.0	56		-0.44	-0.75	0.86	s	18.63	1.285	121	121	21:34:10.30	-1:53:17.2
266	PKS2134+004	7.59	12.38	0.79	102	21:34:05.21	0:28:25.1	56		-0.58	0.28	0.65	s	16.53	1.937	110	4	21:36:38.58	0:41:54.3
267	PKS2135-248	0.77	0.69	-0.18	7	21:35:45.40	-24:53:28.5	57		0.10	-0.39	0.40	s	17.29	0.821	107	108	21:38:37.18	-24:39:54.5
268	PKS2140-048	0.77	0.60	-0.40	7	21:39:59.96	-4:51:27.8	57		0.18	-0.35	0.39	s	17.13	0.344	112	0	21:42:36.89	-4:37:43.5
269	PKS2143-156	1.11	0.82	-0.49	7	21:43:38.87	-15:39:37.3	56		0.34	-0.31	0.46	s	17.24	0.698	121	121	21:46:22.97	-15:25:43.8
270	PKS2144+092	0.95	1.01	0.10	79	21:44:42.47	9:15:51.2	56		-0.34	0.20	0.39	s	18.66	1.113	105	0	21:47:10.15	9:29:46.8
271	PKS2145+067	3.30	4.50	0.50	-79	21:45:36.08	6:43:40.9	56		-0.60	-0.40	0.72	s	16.75	0.999	84	84	21:48:05.45	6:57:38.7
272	PKS2145-176	0.82	0.79	-0.06	-7	21:45:51.48	-17:37:42.3	121		1.86	-0.41	1.91	s	20.24	2.130	121	121	21:48:36.80	-17:23:43.5
273	PKS2149-307	1.32	1.15	-0.22	78	21:49:00.59	-30:42:00.2	56		-0.54	-0.83	0.99	s	17.69	2.345	107	108	21:51:55.52	-30:27:53.7
274	PKS2149+069	0.89	0.94	0.09	79	21:49:02.10	6:55:21.0	60		-0.59	-0.30	0.66	s	18.64	1.364	112	0	21:51:31.45	7:09:27.0
275	PKS2149+056	1.01	1.19	0.27	79	21:49:07.70	5:38:06.9	57	(K)	0.24	0.52	0.57	f	0.00	0.740	86	86	21:51:37.87	5:52:13.1
276	PKS2155-152	1.67	1.58	-0.09	-7	21:55:23.24	-15:15:30.2	56		-0.39	-0.14	0.41	s	18.15	0.672	87	87	21:58:06.28	-15:01:09.3
277	PKS2200-238	0.53	0.46	-0.23	103	22:00:07.71	-23:49:41.1	121		-0.52	-0.99	1.12	s	17.73	2.120	107	108	22:02:55.99	-23:35:09.7
278	PKS2203-188	5.25	4.24	-0.35	103	22:03:25.73	-18:50:17.1	56		0.05	-0.12	0.13	s	18.55	0.619	107	108	22:06:10.41	-18:35:38.7
279	PKS2206-237	1.33	0.98	-0.50	103	22:06:32.63	-23:46:38.2	121		0.77	-1.35	1.56	g	17.65	0.0863	15	108	22:09:20.15	-23:31:53.2
280	PKS2208-137	0.72	0.53	-0.50	103	22:08:42.93	-13:43:00.0	121		-1.92	1.50	2.43	s	16.79	0.392	64	64	22:11:24.16	-13:28:10.8

© 0000	name	$S_{2.7}$	$S_{5.0}$	$\alpha$	Rf	RA(B1950)	Dec(B1950)	Rc	comment	$\Delta$ RA	$\Delta$ Dec	$\Delta$ r	cl	$B_J$	z	Rz	Rsp	RA(J2000)	Dec(J2000)
281	PKS2210-257	0.96	1.02	0.10	103	22:10:14.13	-25:44:22.5	56		-1.70	-1.12	2.03	s	17.86	1.833	107	108	22:13:02.50	-25:29:30.1
282	PKS2212-299	0.54	0.44	-0.33	103	22:12:25.11	-29:59:19.8	121		-0.44	-0.24	0.50	s	17.24	2.703	5	5	22:15:16.03	-29:44:23.0
283	PKS2215+020	0.70	0.64	-0.15	102	22:15:15.59	2:05:09.0	57		-0.74	-0.50	0.89	s	21.97	3.572	121	121	22:17:48.24	2:20:10.9
284	PKS2216-038	1.04	1.30	0.36	102	22:16:16.38	-3:50:40.7	56		-0.23	-0.38	0.45	s	16.65	0.901	109	109	22:18:52.03	-3:35:36.8
285	PKS2223-052	4.70	4.31	-0.14	103	22:23:11.08	-5:12:17.8	57		0.64	-0.30	0.71	s	17.12	1.404	73	0	22:25:47.26	-4:57:01.3
286	PKS2227-088	1.49	1.41	-0.09	103	22:27:02.34	-8:48:17.6	56		1.20	0.02	1.20	s	18.05	1.561	107	108	22:29:40.08	-8:32:54.3
287	PKS2227-399	1.02	1.02	0.00	6	22:27:44.98	-39:58:16.8	56		-0.71	-0.62	0.94	s	17.41	0.323	71	-71	22:30:40.27	-39:42:52.0
288	PKS2229-172	0.52	0.58	0.18	103	22:29:41.00	-17:14:29.6	121		0.24	-1.26	1.28	f	21.28	1.780	121	121	22:32:22.56	-16:59:01.8
289	PKS2233-148	0.50	0.61	0.32	103	22:33:53.98	-14:48:56.7	57		-0.78	0.07	0.78	s	20.85	>0.609	-121	121	22:36:34.08	-14:33:22.1
290	PKS2239+096	0.65	0.70	0.12	79	22:39:19.85	9:38:09.9	56		-0.49	1.20	1.29	s	19.73	1.707	105	0	22:41:49.72	9:53:52.6
291	PKS2240-260	1.08	1.00	-0.12	103	22:40:41.84	-26:00:15.9	120		-0.77	-0.72	1.05	s	17.87	0.774	88	108	22:43:26.42	-25:44:29.0
292	PKS2243-123	2.74	2.38	-0.23	103	22:43:39.80	-12:22:40.3	56		0.40	-0.46	0.61	s	16.50	0.63	10	54	22:46:18.23	-12:06:51.2
293	PKS2245+029	0.66	0.58	-0.21	102	22:45:26.02	2:54:51.2	121		0.84	-0.40	0.93	s	19.52	0.0	0	0	22:47:58.67	3:10:42.7
294	PKS2245-328	2.01	1.80	-0.18	78	22:45:51.50	-32:51:44.3	121		0.11	0.63	0.64	s	18.24	2.268	59	108	22:48:38.68	-32:35:51.9
295	PKS2252-090	0.63	0.69	0.15	103	22:52:27.49	-9:00:04.6	57	(K)	-0.34	-0.40	0.53	s	0.00	0.6064	121	121	22:55:04.23	-8:44:03.8
296	PKS2254-367	0.82	0.72	-0.21	6	22:54:23.11	-36:43:47.4	121		-0.18	0.24	0.30	g	11.41	0.0055	121	121	22:57:10.61	-36:27:44.0
297	PKS2255-282	1.38	1.73	0.37	103	22:55:22.46	-28:14:25.6	57		0.44	0.64	0.77	s	16.61	0.925	107	108	22:58:05.96	-27:58:21.1
298	PKS2300-189	0.98	0.89	-0.16	103	23:00:23.48	-18:57:35.8	121	(mrgDSS)	-0.61	0.09	0.62	m	18.46	0.129	19	19	23:03:02.98	-18:41:25.6
299	PKS2301+060	0.52	0.54	0.06	79	23:01:56.29	6:03:56.9	121		-0.01	-0.20	0.20	s	17.69	1.268	105	0	23:04:28.28	6:20:08.5
300	PKS2303-052	0.54	0.45	-0.30	103	23:03:40.15	-5:16:01.8	121		0.18	-0.08	0.20	s	18.32	1.136	107	108	23:06:15.35	-4:59:48.2
301	PKS2304-230	0.59	0.51	-0.24	103	23:04:58.32	-23:04:08.0	121	(K)	-0.28	0.09	0.30	f	0.00	0.0	0	0	23:07:38.65	-22:47:53.0
302	PKS2312-319	0.71	0.58	-0.33	78	23:12:06.37	-31:55:00.6	121		-0.75	-1.31	1.51	s	17.60	1.323	121	121	23:14:48.49	-31:38:38.7
303	PKS2313-438	0.86	0.69	-0.36	6	23:13:34.82	-43:54:10.2	121		-0.50	0.66	0.83	s	19.01	1.847	105	0	23:16:21.09	-43:37:47.0
304	PKS2314-409	0.50	0.42	-0.28	6	23:14:02.01	-40:57:44.4	39		-1.85	-1.46	2.36	s	18.20	2.448	38	0	23:16:46.94	-40:41:20.8
305	PKS2318+049	1.23	1.17	-0.08	79	23:18:12.13	4:57:23.5	56		-0.16	0.00	0.16	s	18.65	0.622	75	0	23:20:44.85	5:13:50.1
306	PKS2320+079	0.70	0.68	-0.05	-79	23:20:03.91	7:55:33.6	55		-0.23	0.10	0.25	s	17.65	2.090	111	0	23:22:36.09	8:12:01.6
307	PKS2325-150	0.63	0.71	0.19	103	23:25:11.60	-15:04:27.3	57		0.97	-0.62	1.15	s	19.50	2.465	107	108	23:27:47.96	-14:47:55.6
308	PKS2329-162	0.98	1.03	0.08	103	23:29:02.40	-16:13:30.8	121		-2.05	-1.22	2.39	s	20.87	1.155	107	108	23:31:38.65	-15:56:56.8
309	PKS2329-384	0.77	0.67	-0.23	6	23:29:18.94	-38:28:21.7	121		0.63	0.45	0.78	s	17.08	1.202	36	108	23:31:59.46	-38:11:47.4
310	PKS2329-415	0.51	0.47	-0.13	6	23:29:37.82	-41:35:12.6	121		0.67	-0.69	0.96	s	18.20	0.671	121	121	23:32:19.04	-41:18:38.1
311	PKS2330+083	0.52	0.57	0.15	79	23:30:25.06	8:21:36.1	121	(K)	0.33	-0.42	0.53	f	0.00	0.0	0	0	23:32:57.60	8:38:10.7
312	PKS2331-240	1.04	1.06	0.03	103	23:31:17.98	-24:00:15.6	56		-0.83	-0.42	0.93	g	16.47	0.0477	112	108	23:33:55.27	-23:43:40.3
313	PKS2332-017	0.64	0.53	-0.31	102	23:32:46.42	-1:47:45.3	121		-0.41	-0.45	0.61	s	18.41	1.184	110	4	23:35:20.41	-1:31:09.4
314	PKS2335-181	0.69	0.59	-0.25	103	23:35:20.65	-18:08:57.6	121	Do -note	0.30	-0.55	0.63	s	16.76	1.450	121	121	23:37:56.63	-17:52:20.4
315	PKS2335-027	0.60	0.65	0.13	102	23:35:23.25	-2:47:34.5	57		0.51	0.29	0.59	s	18.06	1.072	110	4	23:37:57.33	-2:30:57.4
316	PKS2337-334	1.36	1.17	-0.24	78	23:37:16.67	-33:26:54.8	57	(R)	0.06	-0.04	0.07	f	0.00	0.0	0	0	23:39:54.53	-33:10:16.7
317	PKS2344+092	1.60	1.42	-0.19	-79	23:44:03.77	9:14:05.5	56		-0.42	-0.50	0.65	s	16.15	0.6726	95	95	23:46:36.83	9:30:45.7
318	PKS2344-192	0.54	0.43	-0.37	103	23:44:33.44	-19:12:59.1	121	(R)	-0.61	-0.58	0.84	f	0.00	0.0	0	0	23:47:08.63	-18:56:18.6
319	PKS2345-167	4.08	3.47	-0.26	103	23:45:27.69	-16:47:52.6	56		0.96	-0.62	1.14	s	17.32	0.576	93	93	23:48:02.61	-16:31:11.9
320	PKS2351-006	0.51	0.47	-0.13	102	23:51:35.39	-0:36:29.5	121		-2.05	-0.75	2.18	s	18.05	0.464	110	28	23:54:09.17	-0:19:47.7
321	PKS2351-154	1.08	0.93	-0.24	103	23:51:55.88	-15:29:53.0	57		-1.98	-0.65	2.09	s	18.65	2.6750	94	5	23:54:30.19	-15:13:11.1
322	PKS2354-117	1.57	1.39	-0.20	103	23:54:57.20	-11:42:21.1	121	Do+CC	-1.28	-1.42	1.91	s	17.80	0.960	105	0	23:57:31.19	-11:25:38.9
323	PKS2358-161	0.50	0.37	-0.49	103	23:58:31.56	-16:07:49.1	121		-1.31	-0.77	1.52	s	18.28	2.033	107	108	0:01:05.34	-15:51:06.7

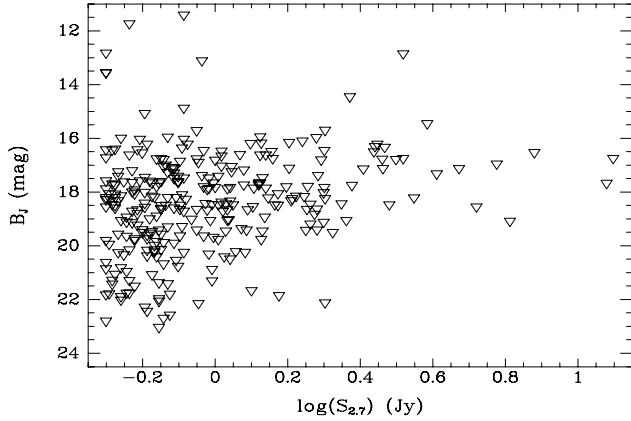


**Figure 9.** The distribution of  $B_J$  magnitudes as a function of 2.7 GHz radio flux for all sources in the survey.

This correlation can be modelled by assuming a strict proportionality between the  $B_J$  and 2.7 GHz luminosities of our quasars, but adding the light of a host galaxy. If we assume that all host galaxies have absolute  $B_J$  magnitudes of  $\sim -20.5$ , the quasar light will dominate over the host galaxy light for 2.7 GHz luminosities  $> 10^{26} \text{W Hz}^{-1}$  (for assumed cosmology see the caption to Fig. 10). Above this luminosity there will be no correlation between  $R$  and the radio flux, as observed, and below this luminosity  $R$  will be proportional to the radio flux, which is consistent with the observed correlation.

The radio spectral indices do not correlate with redshift, apparent  $B_J$  magnitude, radio flux or radio luminosity—but the range of spectral index in the sample is of course limited.

## ACKNOWLEDGEMENTS

The compilation of this paper would not have been possible without the efforts of many people who have worked on the Parkes radio samples over the past 20 years or more. We particularly acknowledge the work done by Graeme White on the optical identifications, Saul Caganoff on the early stages of our image analysis, and Alan Wright and Robina Otrupcek in compiling the machine-readable version of the Parkes Catalogue.

Our new radio observations were made with the VLA and the ATCA. John Reynolds and Lucyna Kedziora-Chudczer assisted with the ATCA observations and we would also like to thank John Reynolds for helpful comments about astrometry.

We would like to thank Raylee Stathakis for making our service observations on the AAT, Russell Cannon, Director of the AAO for awarding us additional discretionary observing time and Roy Antaw for extracting large amounts of data from the AAT archive for us. We are also grateful to Katrina Sealey for obtaining some additional data for us with the ANU 2.3m Telescope and Mike Bessell for giving technical advice about the 2.3m out-of-hours.

We have made substantial use of the following on-line databases in the compilation of this paper: The APM Catalogues (we thank Mike Irwin for scanning ad-

ditional fields for us); the Center for Astrophysics Redshift Survey (with kind assistance from Cathy Clemens); the COSMOS/UKST Southern Sky Catalogue supplied by the Anglo-Australian Observatory; the Lyon-Meudon Extragalactic Database (LEDA) supplied by the LEDA team at the CRAL-Observatoire de Lyon (France); the NASA/IPAC Extragalactic Database (NED) which is operated by the Jet Propulsion Laboratory, Caltech, under contract with the National Aeronautics and Space Administration.

The Digitized Sky Survey was produced at the Space Telescope Science Institute under U.S. Government grant NAG W-2166. The images are based on photographic data obtained using the Oschin Schmidt Telescope on Palomar Mountain and the UK Schmidt Telescope. The plates were processed into compressed digital form with the permission of these institutions.

The Palomar Observatory Sky Survey was funded by the National Geographic Society. The Oschin Schmidt Telescope is operated by the California Institute of Technology and Palomar Observatory.

The UK Schmidt Telescope was operated by the Royal Observatory Edinburgh, with funding from the UK Science and Engineering Research Council, until 1988 June, and thereafter by the Anglo-Australian Observatory. Original plate material is copyright the Royal Observatory Edinburgh and the Anglo-Australian Observatory.

Finally we wish to thank the referee for many helpful suggestions.

## REFERENCES

This section lists the references in alphabetical order, each followed by a code number used to refer to the reference in Table 5.

- Baars, J. W. M., Genzel, R., Pauliny-Toth, I. I. K., Witzel, A., 1977, *A&A*, 61, 99 (001)  
 Baldwin, J. A., 1975, *ApJ*, 201, 26 (002)  
 Baldwin, J. A., Wampler, E. J., Burbidge, E. M., 1981, *ApJ*, 243, 76 (003)  
 Baldwin, J. A., Wampler, E. J., Gaskell, C. M., 1989, *ApJ*, 338, 630 (004)  
 Barthel, P. D., Tytler, D. R., Thomson, B., 1990, *A&AS*, 82, 339 (005)  
 Bolton, J. G., Shimmins, A. J., 1973, *Aust. J. Phys., Astrophys. Suppl.*, 30, 1 (006)  
 Bolton, J. G., Shimmins, A. J., Wall, J. V., 1975, *Aust. J. Phys., Astrophys. Suppl.*, 34, 1 (007)  
 Bolton, J. G., Savage, A., Wright, A. E., 1979, *Aust. J. Phys., Astrophys. Suppl.*, 46, 1 (008)  
 Browne, I. W. A., Wright, A. E., 1985, *MNRAS*, 213, 97 (009)  
 Browne, I. W. A., Savage, A., Bolton, J. G., 1975, *MNRAS*, 173, 87p (010)  
 Burbidge, E. M., 1967, *ApJ*, 149, L51 (011)  
 Burbidge, E. M., 1968, *ApJ*, 154, L109 (012)  
 Burbidge, E. M., Rosenberg, F. D., 1965, *ApJ*, 142, 1673 (013)  
 Burbidge, E. M., Strittmatter, P. A., 1972, *ApJ*, 174, L57 (014)  
 Caganoff, S., 1989, Ph. D. Thesis. Australian National University, Canberra (015)

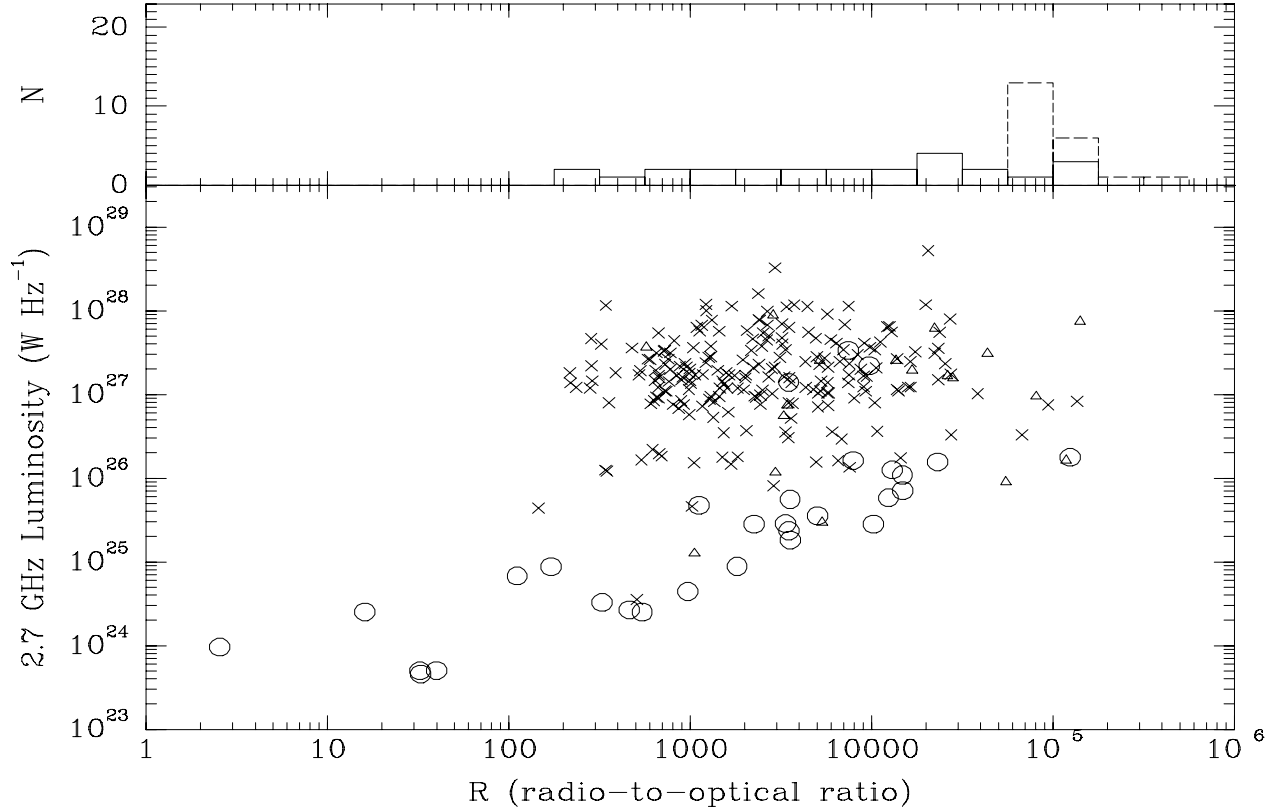


**Figure 10.** Radio-to-optical ratios  $R$  as a function of 2.7 GHz luminosity. Absolute magnitudes and luminosities were computed assuming  $H_0 = 75 \text{ km s}^{-1} \text{ Mpc}^{-1}$  and  $q_0 = 0.5$ ;  $B_J$  magnitudes were  $K$ -corrected assuming a continuum slope of  $f_\nu \propto \nu^{-1}$ , and radio slope  $f_\nu \propto \nu^{-0.09}$  which is the median slope of our sources. Morphologically extended sources (as classified automatically) are marked as circles and unresolved sources as crosses; faint and merged sources are indicated by triangles. Radio-to-optical ratios of sources without measured redshifts are presented as a histogram in the top panel; dotted lines show lower limits on radio-to-optical ratios for sources not detected on the sky surveys.

- Condon, J. J., Broderick, J. J., Seielstad, G. A., 1991, *AJ*, 102, 2041 (016)
- Condon, J. J., Hicks, P. D., Jauncey, D. L., 1977, *AJ*, 82, 692 (017)
- Da Costa, L. N., Nunes, M. A., Pellegrini, P. S., Willmer, C., Chincarini, G., Cowen, J. J., 1986, *AJ*, 91, 6 (018)
- Danziger, I. J., Goss, W. M., 1983, *MNRAS*, 202, 703 (019)
- Dekker, H., D'Odorico, S., 1984, *Messenger*, no. 37, 7 (020)
- de Vaucouleurs, G., de Vaucouleurs, A., Corwin Jr., H. G., Buta, R. J., Paturel, G., Fouqué, P., 1991, *Third Reference Catalogue of Bright Galaxies*. Springer-Verlag, New York (021)
- Downes, A. J. B., Peacock, J. A., Savage, A., Carrie, D. R., 1986, *MNRAS*, 218, 31 (022)
- Drinkwater, M. J., Schmidt, R. W., 1996, *PASA*, 13, 127 (023)
- Drinkwater, M. J., Barnes, D. G., Ellison, S. L., 1995, *PASA*, 12, 248 (024)
- Dunlop, J. S., Peacock, J. A., Savage, A., Lilly, S. J., Heasley, J. N., Simon, A. J. B., 1989, *MNRAS*, 238, 1171 (025)
- Fairall, A. P. et al., 1992, *AJ*, 103, 11 (026)
- Fiedler, R. L. et al., 1987, *ApJS*, 65, 319 (027)
- Foltz, C. B., Chaffee, F. H., Hewett, P. C., Weymann, R. J., Anderson, S. F., MacAlpine, G. M., 1989, *AJ*, 98, 1959 (028)
- Helou, G., Madore, B. F., Schmitz, M., Bica, M. D., Wu, X., Bennett, J., 1991, in Egret, D., Albrecht, M., eds, *Databases and On-Line Data in Astronomy*. Kluwer, Dordrecht, p. 89 (029)
- Hewett, P. C., Foltz, C. B., Chaffee, F. H., Francis, P. J., Weymann, R. J., Morris, S. L., Anderson, S. F., MacAlpine, G. M., 1991, *AJ*, 101, 1121 (030)
- Hewett, P. C., Foltz, C. B., Chaffee, F. H., 1995, *AJ*, 109, 1498 (031)
- Hewett, A., Burbidge, G., 1993, *ApJS*, 87, 451 (032)
- Huchra, J., Geller, M., Clemens, C., Tokarz, S., Michel, A., 1992, *Bull. Inf. Cent. Données Astron. Strasb.* 41, 31 (033)
- Hunstead, R. W., Murdoch, H. S., Shobbrook, R. R., 1978, *MNRAS*, 185, 149 (034)
- Irwin, M., Maddox, S., McMahon, R., 1994, *Spectrum: Newsletter of the Royal Observatories*, no. 4, 14 (035)
- Jauncey, D. L., Wright, A. E., Peterson, B. A., Condon, J. J., 1978, *ApJ*, 219, L1 (036)
- Jauncey, D. L., Batty, M. J., Gulkis, S., Savage, A., 1982, *AJ*, 87, 763 (037)

- Jauncey, D. L., Batty, M. J., Wright, A. E., Peterson, B. A., Savage, A., 1984, *ApJ*, 286, 498 (038)
- Jauncey, D. L., Savage, A., Morabito, D. D., Preston, R. A., Nicholson, G. D., Tzioumis, A. K., 1989, *AJ*, 98, 54 (039)
- Johnston, K. J. et al., 1995, *AJ*, 110, 880 (040)
- Kühr, H., Witzel, A., Pauliny-Toth, I. I. K., Nauber, U., 1981, *A&AS*, 45, 367 (041)
- Laing, R. A., Riley, J. M., Longair, M. S., 1983, *MNRAS*, 204, 151 (042)
- Lister, M. L., Gower, A. C., Hutchings, J. B., 1994, *AJ*, 108, 821 (043)
- Lynds, C. R., 1967, *ApJ*, 147, 837 (044)
- Ma, C., Shaffer, D. B., De Veegt, C., Johnston, K. J., Russell, J. L., 1990, *AJ*, 99, 1284 (045)
- Maoz, D. et al., 1993, *ApJ*, 409, 28 (046)
- Maza, J., Ruiz, M.-T., 1989, *ApJS*, 69, 353, (047)
- Melnick, J., Quintana, H., 1981, *AJ*, 86, 1567 (048)
- Metcalfe, N., Fong, R., Shanks, T., Kilkenny, D., 1989, *MNRAS*, 236, 207 (049)
- Morabito, D. D., Preston, R. A., Slade, M. A., Jauncey, D. L., 1982, *AJ*, 87, 517 (050)
- Morris, S. L., Ward, M. J., 1988, *MNRAS*, 230, 639 (051)
- Morton, D. C., Savage, A., Bolton, J. G., 1978, *MNRAS*, 185, 735 (052)
- Murdoch, H. S., Hunstead, R. W., White, G. L., 1984., *PASA*, 5, 341 (053)
- Oke, J. B., Shields, G. A., Korycansky, D. G., 1984, *ApJ*, 277, 64 (054)
- Patnaik, A., 1996, in preparation (055)
- Perley, R. A., 1982, *AJ*, 87, 859 (056)
- Perley, R.A., Taylor, G.B., 1996, *The VLA Calibrator Manual*. National Radio Astronomy Observatory, Socorro (057)
- Peterson, B. A., Jauncey, D. L., Wright, A. E., Condon, J. J., 1976, *ApJ*, 207, L5 (058)
- Peterson, B. A., Wright, A. E., Jauncey, D. L., Condon, J. J., 1979, *ApJ*, 232, 400 (059)
- Preston, R. A., Morabito, D. D., Williams, J. G., Faulkner, J., Jauncey, D. L., Nicholson, G. D. 1985, *AJ*, 90, 1599 (060)
- Röser, S., Bastian, U., Kuzmin, A., 1994, *A&AS*, 105, 301 (061)
- Reynolds, J. E. et al., 1995, *A&A*, 304, 116 (062)
- Richstone, D. O., Schmidt, M., 1980, *ApJ*, 235, 361 (063)
- Russell, J. L. et al., 1994, *Astron. J.*, 107, 379 (064)
- Sandage, A., 1966, *ApJ*, 145, 1 (065)
- Sargent, W. L. W., 1970, *ApJ*, 160, 405 (066)
- Sargent, W. L. W., Schechter, P. L., Boksenberg, A., Shortridge, K., 1977, *ApJ*, 212, 326 (067)
- Sargent, W. L. W., Steidel, C. C., Boksenberg, A., 1989, *ApJS*, 69, 703 (068)
- Savage, A., Browne, I. W. A., Bolton, J. G., 1976, *MNRAS*, 177, 77p (069)
- Savage, A., Wright, A. E., Bolton, J. G., 1977, *Aust. J. Phys., Astrophys. Suppl.*, 44, 1 (070)
- Savage, A., Clowes, R. G., Cannon, R. D., Cheung, K., Smith, M. G., Boksenberg, A., Wall, J. V., 1985, *MNRAS*, 213, 485 (071)
- Savage, A., Jauncey, D. L., White, G. L., Peterson, B. A., Peters W. L., Gulkis, S., Condon, J. J., 1990, *Aust. J. Phys.*, 43, 241 (072)
- Schmidt, M., 1966, *ApJ*, 144, 443 (073)
- Schmidt, M., 1970, *ApJ*, 162, 371 (074)
- Schmidt, M., 1977, *ApJ*, 217, 358 (075)
- Schmidt, M., Green, R. F., 1983, *ApJ*, 269, 352 (076)
- Shepherd, M. C., Pearson, T. J., Taylor, G. B., 1995, *BAAS*, 27, 903 (077)
- Shimmins, A. J., Bolton, J. G., 1974, *Aust. J. Phys., Astrophys. Suppl.*, 32, 1 (078)
- Shimmins, A. J., Bolton, J. G., Wall, J. V., 1975, *Aust. J. Phys., Astrophys. Suppl.*, 34, 63 (079)
- Smith, H. E., Jura, M., Margon, B., 1979, *ApJ*, 228, 369 (080)
- Spinrad, H., Liebert, J., Smith, H. E., Hunstead, R. W., 1976, *ApJ*, 206, L79 (081)
- Spinrad, H., Marr, J., Aguilar, L., Djorgovski, S., 1985, *PASP*, 97, 932 (082)
- Stannard, D., Bentley, M., 1977, *MNRAS*, 180, 703 (083)
- Steidel, C. C., Sargent, W. L. W., 1991, *ApJ*, 382, 433 (084)
- Steidel, C. C., Sargent, W. L. W., 1992, *ApJS*, 80, 1 (085)
- Stickel, M., Kühr, H., 1993, *A&AS*, 100, 395 (086)
- Stickel, M., Fried, J. W., Kühr, H., 1989, *A&AS*, 80, 103 (087)
- Stickel, M., Padovani, P., Urry, C. M., Fried, J. W., Kühr, H., 1991, *ApJ*, 374, 431 (088)
- Stickel, M., Kühr, H., Fried, J. W., 1993, *A&AS*, 97, 483 (089)
- Stickel, M., Fried, J. W., Kühr, H., 1993, *A&AS*, 98, 393 (090)
- Stickel, M., Meisenheimer, K., Kühr, H., 1994, *A&AS*, 105, 211 (091)
- Sutherland, W., Saunders, W., 1992, *MNRAS*, 259, 413 (092)
- Tadhunter, C. N., Morganti, R., di Serego Alighieri, S., Fosbury, R. A. E., Danziger, I. J., 1993, *MNRAS*, 263, 999 (093)
- Tytler, D., Fan, X.-M., 1992, *ApJS*, 79, 1 (094)
- Tytler, D., Boksenberg, A., Sargent, W. L. W., Young, P., Kunth, D., 1987, *ApJS*, 64, 667 (095)
- Ulrich, M.-H., 1981, *A&A*, 103, L1 (096)
- Ulvestad, J., Johnston, K., Perley, R., Fomalont, E., 1981, *AJ*, 86, 1010 (097)
- Véron, P., Véron-Cetty, M.-P., Djorgovski, S., Magain, P., Meylan, G., Surdej, J., 1990, *A&AS*, 86, 543 (098)
- Véron-Cetty, M.-P., Véron, P., 1993, *ESO Sci. Rep.*, 13, 1 (099)
- Wall, J. V., 1972, *Aust. J. Phys., Astrophys. Suppl.*, 24, 1 (100)
- Wall, J. V., Peacock, J. A., 1985, *MNRAS*, 216, 173 (101)
- Wall, J. V., Shimmins, A. J., Merckelijn, J. K., 1971, *Aust. J. Phys., Astrophys. Suppl.*, 19, 1 (102)
- Wall, J. V., Wright, A. E., Bolton, J. G., 1976, *Aust. J. Phys., Astrophys. Suppl.*, 39, 1 (103)
- Webster, R. L., Francis, P. J., Peterson, B. A., Drinkwater, M. J., Masci, F. J., 1995, *Nature*, 375, 469 (104)
- White, G. L., Jauncey, D. L., Savage, A., Wright, A. E., Batty, M. J., Peterson, B. A., Gulkis, S., 1988, *ApJ*, 327, 561 (105)
- Wilkes, B. J., 1984, *MNRAS*, 207, 73 (106)
- Wilkes, B. J., 1986, *MNRAS*, 218, 331 (107)
- Wilkes, B. J., Wright, A. E., Jauncey, D. L., Peterson, B. A., 1983, *PASA*, 5, 2 (108)

- Wills, B. J., Netzer, H., Uomoto, A. K., Wills, D., 1980, ApJ, 237, 319 (109)
- Wills, D., Lynds, R., 1978, ApJS, 36, 317 (110)
- Wills, D., Wills, B. J., 1974, ApJ, 190, 271 (111)
- Wills, D., Wills, B. J., 1976, ApJS, 31, 143 (112)
- Wright, A. E., Otrupcek, R. E., 1990, Parkes Catalogue. Australia Telescope National Facility, Epping (PKSCAT90) (113)
- Wright, A. E., Jauncey, D. L., Peterson, B. A., Condon, J. J., 1977, ApJ, 211, L115 (114)
- Wright, A. E., Peterson, B. A., Jauncey, D. L., Condon, J. J., 1978, ApJ, 226, L61 (115)
- Wright, A. E., Peterson, B. A., Jauncey, D. L., Condon, J. J., 1979, ApJ, 229, 73 (116)
- Wright, A. E., Ables, J. G., Allen, D. A., 1983, MNRAS, 205, 793 (117)
- Yentis, D.J., Cruddace, R.G., Gursky, H., Stuart, B.V., Wallin, J.F., MacGillivray, H.T., Collins, C.A., 1992, in MacGillivray, H.T., Thomson, E.B., eds, Digitised Optical Sky Surveys. Kluwer, Dordrecht, p. 67 (118)
- Young, P., Sargent, W. L. W., Boksenberg, A., 1982, ApJS, 48, 455 (119)
- this paper (ATCA radio data) (120)
- this paper (all optical and VLA radio data) (121)

Please note the following sections are not included in this preprint but may be obtained from my preprint page <http://www.aao.gov.au/local/www/mjd/papers/>.

## APPENDIX A: RADIO IMAGES OF RESOLVED SOURCES

**Figure A1:** Radio images of resolved sources from the sample. There is one negative contour (dotted) shown in each image with the same absolute value but opposite sign as the lowest positive contour. The remaining positive contours are spaced logarithmically, each level a factor of 2 larger than the previous one. The title of each image indicates the level of the lowest positive contour as well as the telescope used: the VLA images are at 4.885 GHz and the ATCA images are at 4.796 GHz.

## APPENDIX B: OPTICAL FINDING CHARTS OF ALL SOURCES

**Figure B1:** Finding charts for all the sources generated from the automated sky catalogues. Images classified automatically as unresolved (stellar) are plotted as filled ellipses on the charts; resolved images (galaxies) are plotted as unfilled ellipses. The charts are a good approximation to the photographic data, but we stress that there can be problems with image merging in crowded fields: close objects (e.g. two stars) can be misclassified as a “merged” object or galaxy. The “Field” code at the bottom of each chart indicates the UKST field number (or the plate number for POSS I) with a prefix describing the type of plate. The prefix “J” indicates UKST  $B_J$  plates measured by COSMOS. For APM data “j” indicates UKST  $B_J$  plates, “O” blue POSS I plates and “E” red POSS I plates.

## APPENDIX C: NEW OPTICAL SPECTRA

(to go on microfiche)